

PART I. THE PHOTOCHROMISM OF MERCURY (II)  
DITHIZONATE AND PART II. THE  
DETERMINATION OF SURFACE  
AREAS OF CAPILLARY  
TUBE REACTORS

By

ANTON ELBERT GOODWIN

Bachelor of Arts  
in Chemistry and Mathematics  
Phillips University  
Enid, Oklahoma  
1958

Master of Science  
Oklahoma State University  
Stillwater, Oklahoma  
1975

Submitted to the Faculty of the  
Graduate College of the  
Oklahoma State University  
in partial fulfillment of  
the requirements for  
the Degree of  
DOCTOR OF PHILOSOPHY  
May, 1988

PART I. THE PHOTOCHROMISM OF MERCURY (II)  
DITHIZONATE AND PART II. THE  
DETERMINATION OF SURFACE  
AREAS OF CAPILLARY  
TUBE REACTORS

Thesis Approved:

*Horacio Mottola*

Thesis Adviser

*E. J. Eisentraum*

*J. Paul Alerten*

*S. L. Furber*

*Norman N. Durham*

Dean of the Graduate College

## PREFACE

This thesis has two unrelated parts, one deals with photochromism of mercury (II) dithizonate and a second deals with the determination of surface area in capillary tubes.

The first part came from Dr. Mottola's interest in photochromism and from my interest in developing a method for determining mercury ion in water. That project appealed to me, as an analytical chemist in industry, because photochromism was a new topic to me and because I was familiar with mercury ion. I knew firsthand about some limitations of determining mercury ion in water, such as a high detection limit in atomic adsorption spectrometry.

The second part of the thesis came about when I changed laboratories at work and had access to a nitrogen gas adsorption analyzer, which measures the surface areas of solids. Dr. Mottola's research group was interested in the surface areas inside chemical reactors of continuous-flow systems. A project using that instrument would not only be useful to them, but it would benefit me in different ways.

The main reason for changing the research project was Dr. Mottola's interest in helping me manage time. While pursuing the advanced degree by Talkback Television, I continued to work as a chemist during the weekdays in Ponca City, Oklahoma, and I conducted research at Oklahoma State University in Stillwater during the weekends. As a consequence, much time during the weekend was spent driving to and from the

university, and after arriving there, much time was spent preparing solutions for experiments; research was very slow. The new project would be conducted in Ponca City.

Two people played important roles in my life and I want to acknowledge them. My wife Betty who waited many weekends while I selfishly pursued research, I thank her, and Dr. Mottola for his efforts, his patience, his time, and the understanding that he gave to help me become a better analytical chemist, I thank him.

## TABLE OF CONTENTS

### PART I: THE PHOTOCHROMISM OF MERCURY (II) DITHIZONATE

Chapter	Page
I. PHOTOCHROMISM . . . . .	2
Definition . . . . .	2
Relationship of Photochemical Reactions. . . . .	4
Reaction Mechanisms. . . . .	5
Wavelength for Irradiation . . . . .	7
II. METAL-CHELATE PHOTOCHROMIC SYSTEMS. . . . .	11
General Information. . . . .	11
Photosubstitution. . . . .	12
Heterolytic Cleavage . . . . .	13
Spiropyrans . . . . .	13
Photoredox . . . . .	15
Tris(2,2'-Bipyridine)Ruthenium (III). . . . .	15
Iron (III) Complex of Pinacol . . . . .	17
Dipotassium Trioxooxalatomolybdenum (VI) Hydrate. . . . .	17
Ni(IV) Dithiocarbamates . . . . .	18
Isomerization. . . . .	19
Zinc Salicylidene-p-Toluidinate . . . . .	19
$K_3[Cr(C_2O_4)_3]$ . . . . .	19
Cis-[Co(en) <sub>2</sub> (H <sub>2</sub> O)Cl] <sup>2+</sup> . . . . .	20
Cis-B'-[Co(trien)(H <sub>2</sub> O)Cl] <sup>2+</sup> . . . . .	20
Metal Dithizonates . . . . .	21
Dithizone the Ligand. . . . .	21
Photochromic Dithizonates . . . . .	22
Spectral and Chemical Properties. . . . .	24
Mercury (II) Dithizonate. . . . .	26
Mechanism of Reaction . . . . .	30
Substituent Effects on Hg(HDz) <sub>2</sub> . . . . .	31
Photochromic Switching. . . . .	32
Photochromic Polymers . . . . .	33
Summary . . . . .	33
III. EXPERIMENTAL. . . . .	34
Equipment. . . . .	34
Calibrating the Oscilloscope Screen. . . . .	36

Chapter	Page
Computer Programs for Data Handling. . . . .	37
Program FAST4 . . . . .	37
Program AMAX-HRDCP. . . . .	39
Reagents and Solutions . . . . .	40
Cleaning of Glassware. . . . .	40
Procedures . . . . .	40
 IV. RESULTS AND DISCUSSION. . . . .	 42
Rate Profile Curves . . . . .	43
The Effect of Dithizone . . . . .	44
The Effect of Irradiation Time. . . . .	47
Mathematical Model . . . . .	47
Sorting Mathematical Models. . . . .	49
Photochromic Method. . . . .	50
 BIBLIOGRAPHY. . . . .	 54
 APPENDIXES	
APPENDIX A - COMPUTER PROGRAM FAST4 . . . . .	58
APPENDIX B - COMPUTER PROGRAM AMAX-HRDCP. . . . .	61
APPENDIX C - DATA USED FOR MODELING PHOTOCHROMISM . . . . .	64
 PART II: THE DETERMINATION OF SURFACE AREAS OF CAPILLARY TUBE REACTORS	
 I. INTRODUCTION. . . . .	 72
II. REACTOR FABRICATION . . . . .	74
Materials. . . . .	74
Glass Reactors and Beads. . . . .	74
Plastic Tubing Reactors . . . . .	74
Procedure for Embedding Control Pore Glass. . . . .	74
III. EXPERIMENTAL. . . . .	76
Equipment. . . . .	76
Overview. . . . .	76
Gas Adsorption Analyzer . . . . .	76
Gas Adsorption Cell . . . . .	78
Design of Gas Adsorption Cell . . . . .	79
Vapor Vent. . . . .	80
Pressure Surge Filters. . . . .	82
Procedure. . . . .	83
The Blank Correction. . . . .	83
The Run Procedure . . . . .	85

Chapter	Page
IV. RESULTS AND DISCUSSION. . . . .	87
Surface Areas. . . . .	87
Langmuir and BET Methods. . . . .	87
Coiled Glass Reactors . . . . .	87
Significance of the Surface Area Value. . . . .	88
Surface Areas for CPG Embedded Reactors . . . . .	91
Surface Areas of Glass Beads. . . . .	95
Summary . . . . .	95
Fractal Dimension. . . . .	96
BIBLIOGRAPHY. . . . .	99

LIST OF TABLES

PART I

Table	Page
1. Mechanism for Photochromic Processes . . . . .	8
2. Photochromic Metal Dithizonates. . . . .	24
3. Physical Values for Hg(HDz) <sub>2</sub> . . . . .	27
4. The Return Rate Coefficients for Dithizonates Reported by Meriwether et al. . . . .	28
5. The Return Rate Coefficients for Dithizonates Reported by Geosling et al. . . . .	29
6. Concentrations of Mercury (II) Dithizonate: Known Concentrations Versus Those Determined by Photochromic Method. . . . .	53

PART II

1. Surface Areas for Various Weights of CPG in a Large Volume (96 mL) Gas Adsorption Cell . . . . .	79
2. Variables and Responses for Determining Blank Cell Correction . . . . .	83
3. 2 <sup>3</sup> Factorial Design for Blank Cell . . . . .	84
4. Isotherms From the 2 <sup>3</sup> Factorial Experiment for the Blank Runs with the Large Volume Cell. . . . .	85
5. Surface Areas for Four Glass Coils . . . . .	88
6. Two Level Factorial Design for 64 mL Cell. . . . .	89
7. 2 <sup>3</sup> Factorial Design for Determining the Surface Area of Coil 1. . . . .	89



Table	Page
8. Isotherms for 2 <sup>3</sup> Factorial Design Experiment to Determine Surface Area of Coil 1 . . . . .	90
9. Calculation of Effects and Mean Squares for Coil 1 by Yates' Method. . . . .	91
10. Surface Areas for Segments of a 2 Meter Teflon Reactor That was Embedded with CPG . . . . .	92
11. Surface Areas for Segments of a 1/2 Meter Teflon Reactor that was Embedded with CPG . . . . .	94
12. Chemical Treatments of Glass Beads . . . . .	96
13. Sieve Designations, Particle Diameter, and Surface Areas for Control Pore Glass Beads (OSU-CPG00075 200/400 Mesh). . . . .	97
14. Sieve Designations, Particle Diameter, and Surface Areas for Control Pore Glass Beads (OSU-CPG03000 200/400 Mesh). . . . .	98

## LIST OF FIGURES

### PART I

Figure	Page
1. Jablonski Diagram to Show Relationships of Physico-Chemical Processes. . . . .	6
2. Experimental Apparatus Used in Studies of Photochromism. . . . .	35
3. The Excited Species Absorbance as a Function of the Ligand to Metal Ratio . . . . .	45
4. Rate Coefficient as a Function of Dithizone Concentration . . . . .	46
5. Logarithmic Plot of the Excited Species Absorbance Versus Time . . . . .	48

### PART II

1. An Automated Gas Adsorption Analyzer for the Determination of Surface Areas. . . . .	77
2. Gas Adsorption Cell for Surface Area Measurements of Capillary Tubes . . . . .	81

PART I

THE PHOTOCHROMISM OF MERCURY

(II) DITHIZONATE

## CHAPTER I

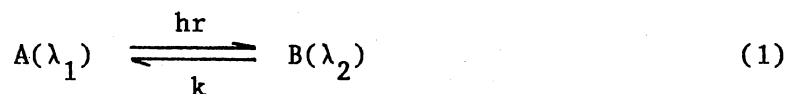
### PHOTOCHROMISM

#### Definition

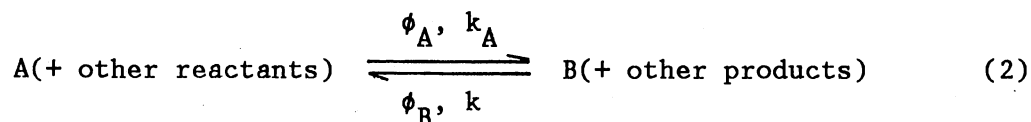
Photochromism and phototropy are terms used to designate a reversible color change induced by light. In 1899 Marckwald (1) used phototropy to describe a phenomenon he observed when either anhydrous quinoquinoline hydrochloride or  $\beta$ -tetrachloro- $\alpha$ -ketonaphthalene became colored by exposure to light and this color faded in the dark. In 1952 while studying low temperature solutions of dianthrone, dianthylene, and xanthylideneanthrone and their derivatives, Hirshberg et al. (2) used the term photochromism to describe the reversible process that takes place when these compounds are irradiated with light. Because phototropy is used by botanists to describe the phenomenon of the alignment of certain plants towards light, then to use photochromism to describe the physicochemical phenomenon would remove some confusion from the literature. Photochromism is used throughout this work.

In 1929 Chalkley (3) expressed difficulty in formulating an exact definition for the process. He hoped that further investigation would find a single distinguishing characteristic that would restrict the term to a fundamentally new phenomenon. He wrote, "the most striking feature is that these color changes are true adaptations," which was an attempt to restrict the phenomenon to a single chemical species. This idea prevailed for years. Brown (4) in 1971 defined photochromism as a

reversible change of a single chemical species between two states having distinguishably different absorption spectra, such change being induced in at least one direction by the action of electromagnetic radiation. His definition is represented by Equation 1.



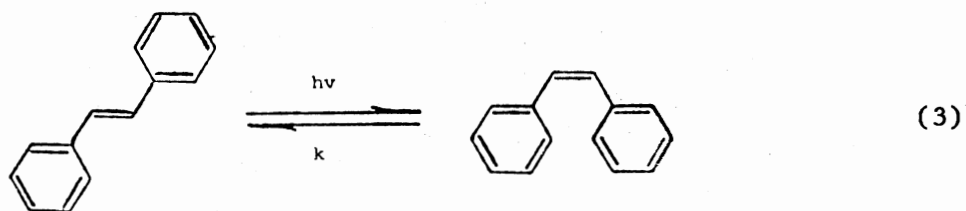
Others have chosen a more general definition which includes processes where more than one chemical species is involved. In 1970 Balzani et al. (5) defined photochromism as a reversible light-induced change of a system between two states having distinguishably different absorption spectra. Adamson (6) in 1975 similarly defined photochromism as being a reversible, light-induced change. He illustrated the process with Equation 2,



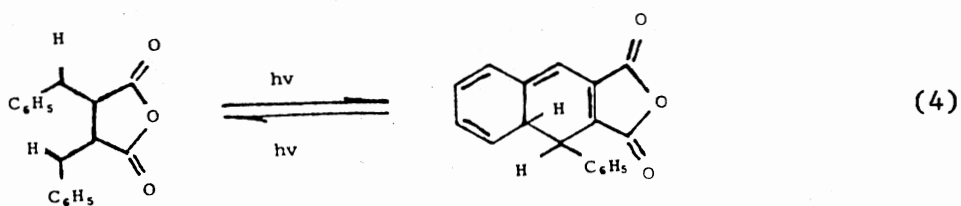
where  $\phi$  denotes the quantum yield for the photochemical reaction and  $k$  denotes the thermal rate coefficients.

Two corollary aspects of Adamson's definition of photochromism are that the reaction be a simple one and that the reaction system be classified as either singly or doubly photochromic. In a simple reaction, the reactants convert to products in a single reaction step and no intermediate or sequential reactions occur. In a singly photochromic system, the forward reaction is photocatalyzed and the return reaction occurs as a thermal process. In a doubly photochromic system, the reaction is photocatalyzed in both directions. Examples of

a singly and doubly photochromic system are the trans-cis isomerization of the stilbenes about a single ethylenic link, Equation 3,



and the tautomerization of fulgides, Equation 4.



$\alpha$ ,  $\delta$ -diphenylfulgide

dihydroderivative

In the latter equation, the forward reaction is induced by UV light and the reverse reaction by visible light. In view of the increasing number of photochromic systems being reported that involve more than one chemical species, the more general definition by Adamson should be accepted.

#### Relationship of Photochemical Reactions

Chalkley (3) in his review pointed out that phosphorescent substances showed color change when exposed to light and reverted to their original color in dark. Yet they were not considered photochromic. To understand the relationship of photochromism with other photochemical and chemical processes, it is helpful to use a Jablonski diagram (see Figure 1). It incorporates Adamson's (6) idea

that a better understanding of photochemical processes results when one recognizes that only excited molecules can have two different excited states. One is the Franck-Condon state where the absorption of a quantum of light produces an electronically excited molecule in an excited vibrational-rotational state. A second state is a thermally equilibrated excited state which has an energy, an entropy, a free energy, a structure, and chemistry. The Franck-Condon state undergoes a radiationless transition to a thermal equilibrated excited state.

While a photochemical reaction is described by Steps 1, 2, 5, and 6 in Figure 1, a thermochemical reaction is described by Steps 4, 5, and 6. The solid line of Step 1 denotes absorption of light to give the Franck-Condon state, and the wavy lines denote radiationless transitions. Similarly, fluorescence and phosphorescence are denoted by the Pathways 1, 2, and 3. While a singly photochromic reaction is denoted by Pathways 1, 2, and 4, and a doubly photochromic reaction uses Steps 1, 2, and 10 and returns by Steps 7, 8, and 11.

#### Reaction Mechanisms

Photochromism occurs in a wide variety of compounds and several different mechanisms have been reported. It is found in inorganic and organic compounds and coordination complexes (3, 4, 6-9). Likewise, photochromism is found in glasses and in living and nonliving systems (10, 11). Table 1 gives examples of different photochromic mechanisms found in the literature and gives a perspective of their range. One obvious observation is the large number of processes due to isomerization. These include heterolytic cleavage, homolytic cleavage, trans-cis isomerization, and tautomerism. Adamson et al. (6) have

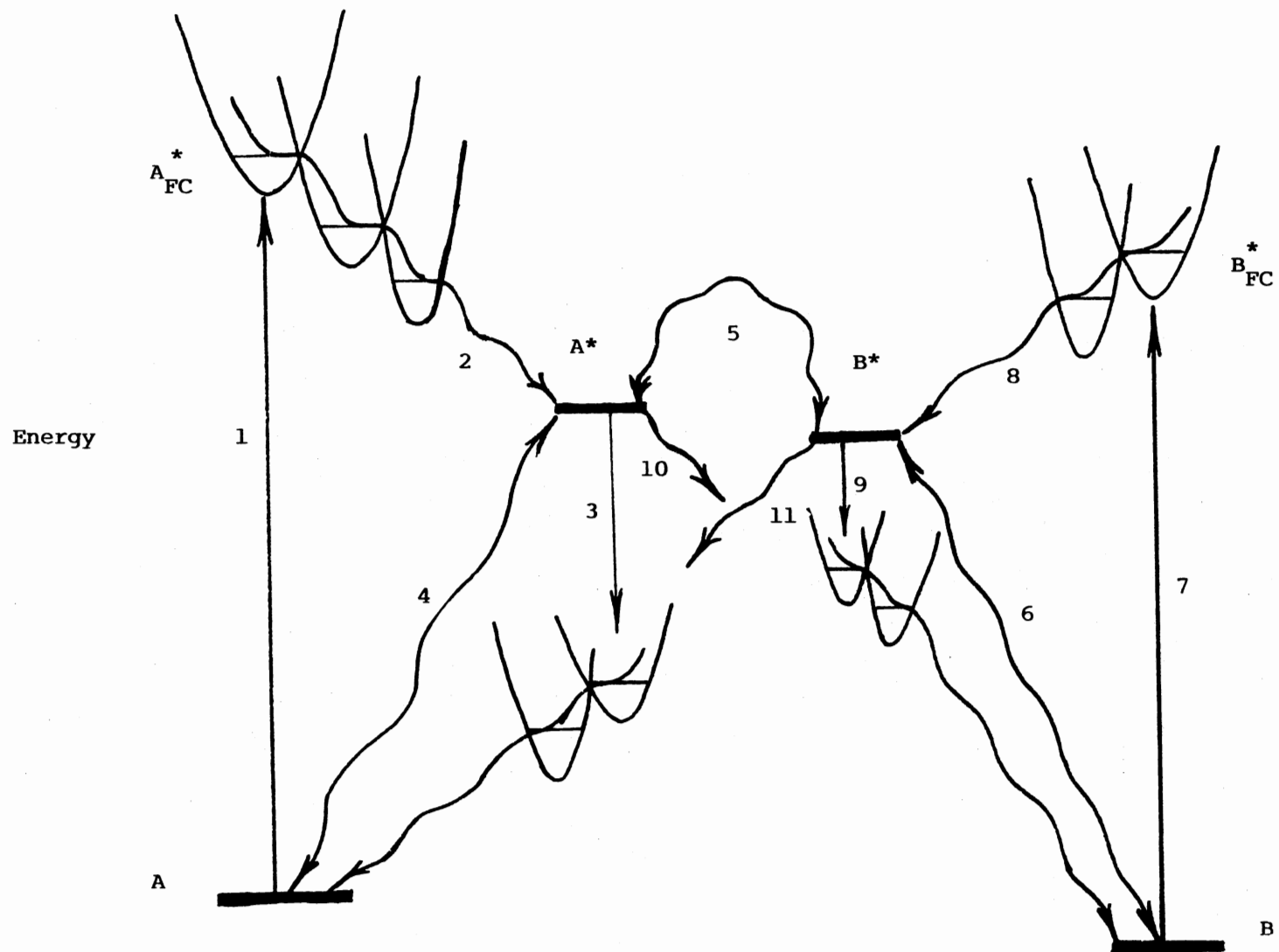


Figure 1. Jablonski Diagram to Show Relationships of Physico-Chemical Processes.



claimed that photoracemization is another photochromic process. Reactions that include more than a single species are photoredox and photosubstitution reactions.

#### Wavelength for Irradiation

Color changes taking place in daylight and darkness, such as observed by Marckwald (1) or Irving (12), focused attention on the phenomenon. As more photochromic compounds were reported, the dependence of the color change on the spectral distribution of the irradiating light was noted. An example in the following paragraph illustrates how complicated this interdependence can be (13).

When irradiated with ultraviolet light from a mercury arc, the compound 2,3-diphenylindenone has an intense red color. When irradiated with an unfiltered light containing visible light from the same source, however, it has a less intense color. Visible light above the wavelength 450 nm does not cause color change of the solutions but speeds up the disappearance of the color.

Two points to be recognized are that each photochromic system should be studied in detail to determine its dependence on the wavelength region of the irradiating light and that photochromism of a compound cannot be excluded until all regions of irradiation have been studied. Other reported wavelength regions of electromagnetic irradiation that bring about photochromism include infrared, X-ray, and gamma irradiation.

TABLE 1  
MECHANISM FOR PHOTOCHROMIC PROCESSES

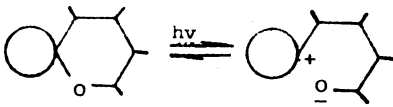
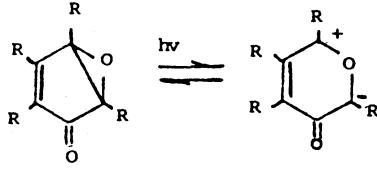
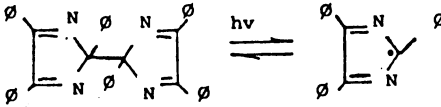
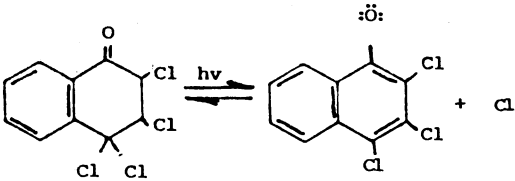
Mechanism	Process
<u>Example</u>	<u>Bond</u>
<u>Heterolytic Cleavage</u>	
Spiroyrans	C-O 
Triarylmethane Dyes	C-N $\text{ArC}^+\text{-NR}_3 \xrightleftharpoons{h\nu} \text{Ar}_3\text{C}^+ + \text{NR}_3$
Indenone Oxides	C-C 
<u>Homolytic Cleavage</u>	
Bis-imidazoles	C-C 
$\alpha$ -tetrachloroketo-dihydronaphthalene	C-Cl 

TABLE 1 (CONTINUED)

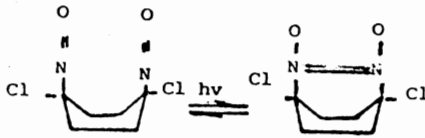
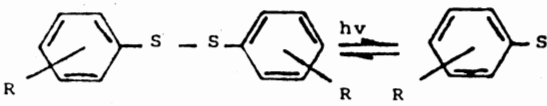
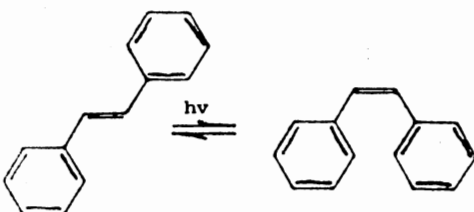
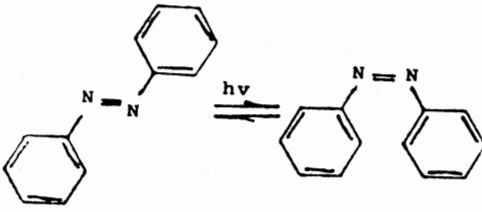
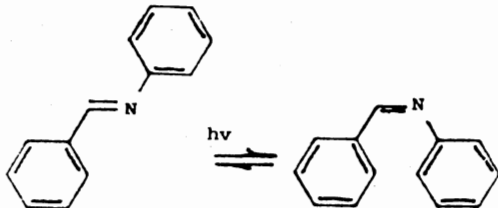
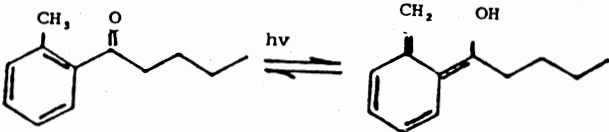
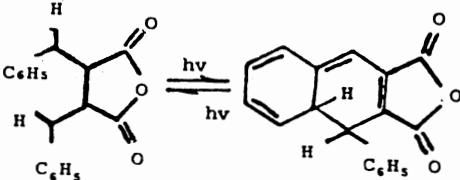
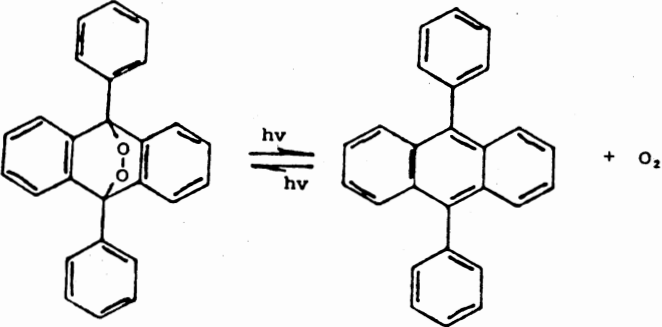
Mechanism	Process
<u>Example</u>	<u>Bond</u>
1,4-dichloro-1,4-dinitrosocyclohexane	N-N 
Aryldisulfide	S-S 
<u>Trans-Cis Isomerization</u>	
Stilbenes	C-C 
Aromatic Azo Compounds	N-N 
Benzalaniline	C-N 

TABLE 1 (CONTINUED)

Mechanism	Process
<u>Example</u>	
<u>Tautomerism</u>	
Ortho-substituted Phenyl Ketones	
Fulgides	
<u>Photoredox</u>	
Endoperoxides	
<u>Photosubstitution</u>	
	$\text{Cr}(\text{H}_2\text{O})_6^{3+} + \text{SCN}^- \xrightleftharpoons{h\nu} \text{Cr}(\text{H}_2\text{O})_5\text{NSC}^{2+} + \text{H}_2\text{O}$

## CHAPTER II

### METAL-CHELATE PHOTOCHROMIC SYSTEMS

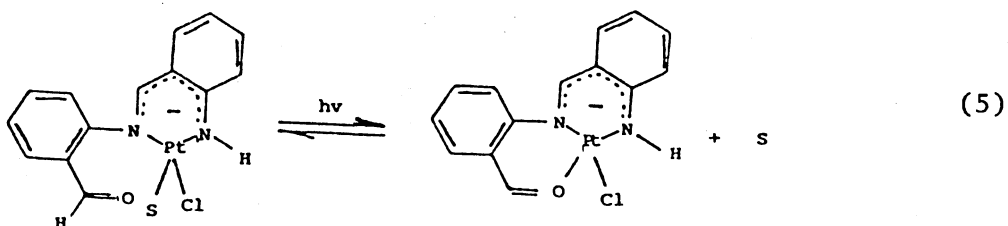
#### General Information

Because color change is the only distinguishing characteristic of the photochromic metal chelates, only a few have been reported. The literature shows the researcher's skepticism for using the photochromic property in an analytical method. Bertelson (14), in 1971, expressed the view that because "wet chemical analysis for trace amounts of metals by solution absorption spectroscopy is rapidly being replaced by atomic absorption and atomic fluorescence spectroscopy ... analytical applications depending on the chemical properties of a photochromic material appear of little practical importance." In 1966 West (15) said "no one has, as yet, made no serious attempts to explore the analytical potentialities of the phenomenon and we have recently turned attention towards it with this view in mind." As of 1980 none of his work on photochromism had appeared in the literature. Sandell and Onishi (16) said "analytically, photochromism is not of importance for the dithizonates of metals other than Hg, Ag, Pd, or Pt."

To better understand the researcher's skepticism, the following sections categorize the photochromic metal-chelates by reaction mechanisms. These include photosubstitution, photoredox, heterolytic cleavage, and isomerization.

## Photosubstitution

Only one photochromic metal-chelate has a reaction mechanism due to photosubstitution. Rohly and Mertes (17) reported the photochromism of platinum (II) with the dimeric condensate of o-aminobenzaldehyde. The process occurs in coordinating solvents, such as acetonitrile and dimethyl sulfoxide; it involves an alternating, solvent-terminal carbonyl occupation of a coordination site. Equation 5 shows this mechanism



where the orange solvated complex turns purple on irradiation with visible light of 420 to 500 nm and ultraviolet light of 250 to 350 nm. The authors thought the reaction was novel and referred to it as a photochromic swinging gate.

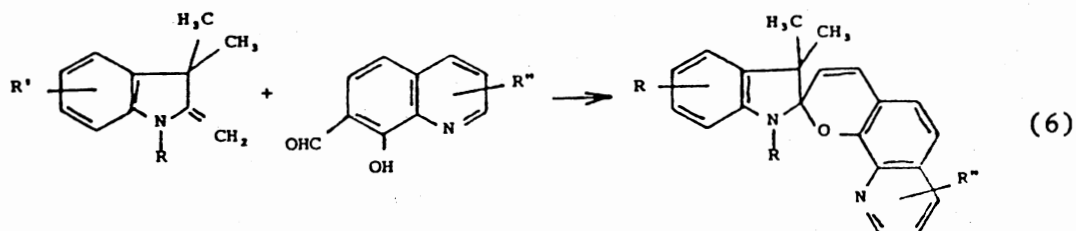
To explain the reaction on the basis of an associative mechanism is to show that the mechanism is not novel. In this mechanism, the square-planar system of platinum when irradiated forms an intermediate with the geometry of a trigonal bipyramid. In this form, the aldehyde group and the solvent molecule are both associated with the platinum atom. This intermediate could also be the excited state of the photochromic process. Because this reaction is reversible, the intermediate does not necessarily proceed to expel the solvent molecule,

which typifies a ligand substitution process. Upon relaxation, the coordinated aldehyde group is dispelled and the complex reverts to the square-planar geometry.

### Heterolytic Cleavage

#### Spiroyrans

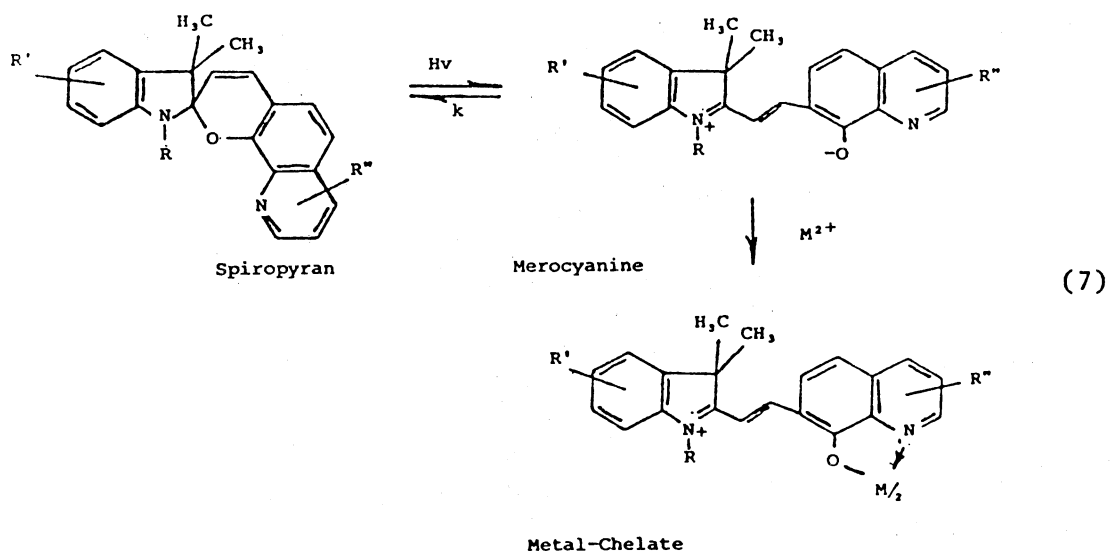
The mechanism for photochromism in spiroyrans is the heterolytic cleavage of a C--O bond (13). Although Phillips et al. (18) succeeded in synthesizing spiroyrans that react with metal ions, the resulting metal-chelates were not photochromic. For example, they reacted various 8-quinolinol aldehydes with 1,3,3-trimethyl 2-methyleneindoline to form spiroyrans. Equation 6 gives a general example of this condensation reaction.



Because of their 8-hydroxyquinolinato structure, these compounds react with Cu(II) and Fe(III) ions at room temperature to give highly-colored solutions. Even at  $-78^{\circ}\text{C}$ , the reactions take place very slowly unless the solublized chelates are irradiated with ultraviolet light.

In 1968 Phillips et al. (19) reported that other substituted aldehydes were used in the same synthesis. They made an important contribution, however, by using the chelating property of 2-[2-(8-hydroxy-7-quinolyl)-vinyl]1,3,3,7-tetramethyl-3H-indolium

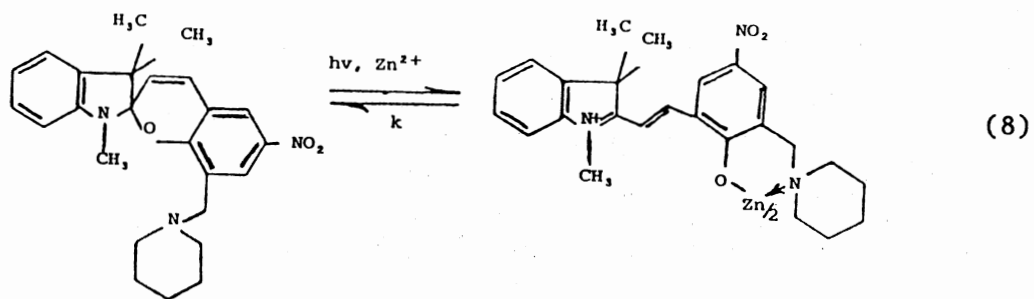
hydroxide inner salt to support the mechanism that the spiroopyran form is colorless and the merocyanine form is colored. Equation 7 shows the relationship of these forms.



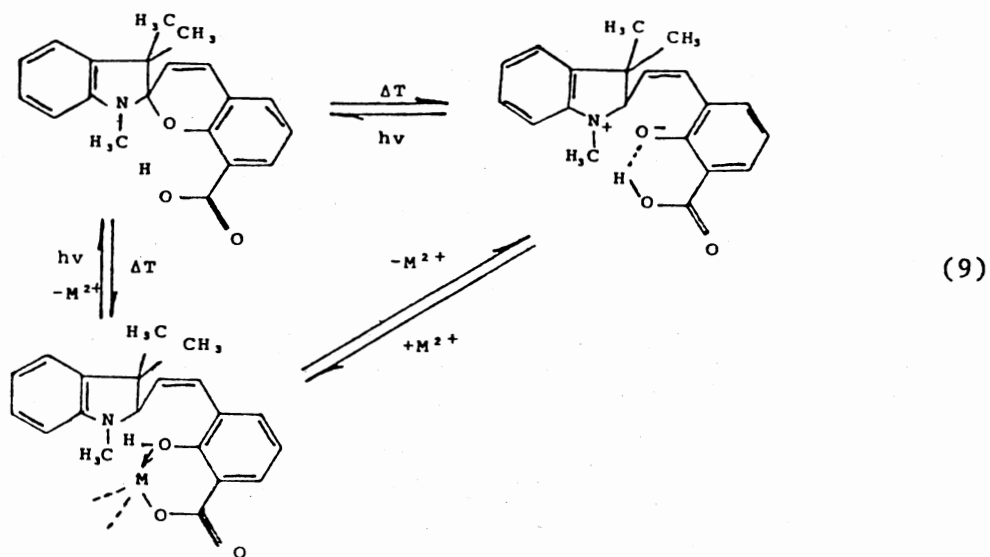
The existence of colorless solutions of this spiropyran in some solvents and the indiscernible difference between the wavelength maxima of both the irradiated ligand and the metal chelates of Ni, Co, Zn, and Cd show the merocyanine form with the chelating center is the excited form. At no time were the metal chelates considered to be photochromic.

But Taylor et al. (20) prepared a spiropyran by reacting 3-hydroxy-methyl-5-nitrosalicylaldehyde with 1,3,3-trimethyl-2-methylene indoline. This compound is a photochromic chelating agent, and it reacts with zinc (II) ion to form a photochromic metal-chelate. Although heating fades the wine-colored complex, irradiating with ultraviolet light regenerates the color. Equation 8 illustrates this photochromic process.





In 1975 Walther and Jager (21) reported that the spiroindoline 1,3,3-trimethyl-spiro(indolin-2-2'-benzopyran)8'-carboxylic acid has inverse photochromism. Both the merocyanine form and the metal-chelate, when irradiated with UV light at room temperature, gave the spiroindoline. A proposed mechanism is given in Equation 9. Five metal ions, Ni(II), Co(II), Cu(II), Zn(II) and Mn(II), are known to react with the compound.

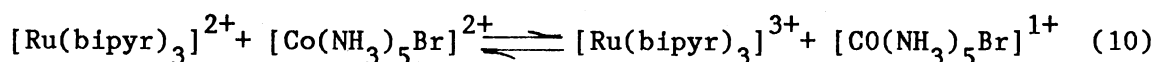


Photoredox

### Tris(2,2'-Bipyridine)Ruthenium (III)

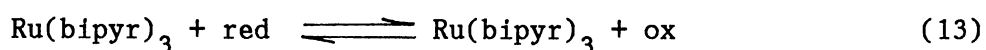
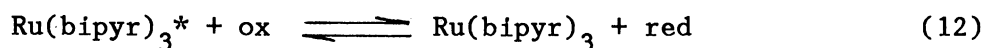
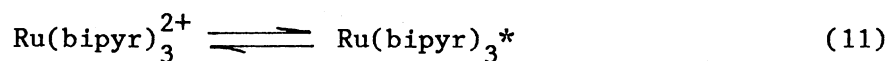
Adamson et al. (6, 22), in 1975, thought that two chemical systems

reported in earlier publications were photochromic. In 1972 he and Gafney (23) had reported a color change from yellow to light green when solutions of  $\{\text{Ru}(\text{bipy})_3\}\text{Cl}_2$  and  $\{\text{Co}(\text{NH}_3)_5\text{Br}\}(\text{NO}_3)_2$  were irradiated at 410 nm. They reported the reaction mechanism as one of electron transfer from the Ru(III) chelate to the Co(II) complex. They gave the following equation:



That the  $\{\text{Ru}(\text{bipy})_3\}^{2+}$  species was regenerated by the addition of sodium acetate suggests, however, that this is not a photochromic process. This process described by Adamson is solvatochromism. Phillips et al. (61-63) have reported that solvatochromic compounds undergo a large variation in color as a function of the polarity of solvents.

In a second example, Adamson claimed that in 1974 he and Bock (24) had worked with a photochromic system. Their publication showed that electron transfer quenching of  $\{\text{Ru}(\text{bipy})_3\}^{2+}$  is an allowed process for both transition metal ion oxidants and electron-deficient organic molecules. The initial quenching reaction was followed by a rapid dark reaction which gives back  $\{\text{Ru}(\text{bipy})_3\}^{2+}$  and the oxidized form of the quencher. The overall reaction is given by the following equations:

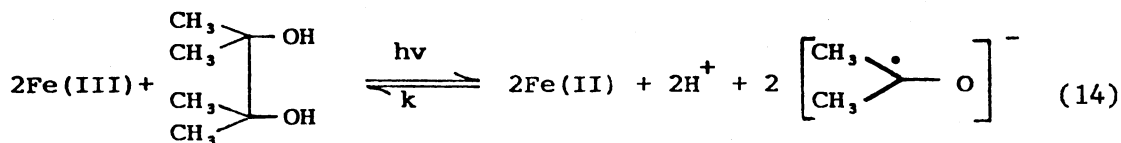


In this example, the reaction is photochromic. The two examples, however, exemplify the confusion that can arise in a reader's mind when

an author claims an earlier discovery of a photochromic system in a later publication. The discovery that is claimed was not realized at the time of the first publication, and it may or may not be substantiated by information that was published then.

#### Iron (III) Complex of Pinacol

After 12 hours of ultraviolet irradiation of solutions of ferric chloride and pinacol, the pale green color returned during the following two weeks (25). The color change was due to the photochemical and thermal redox reactions of the metal complex and is expressed by Equation 14. Because of the long periods of irradiation and relaxation, this reaction would find no use in analytical chemistry.

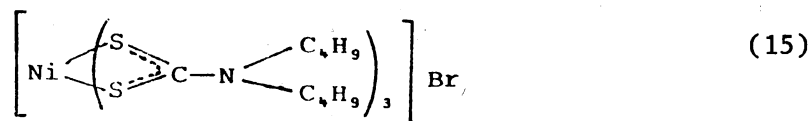


#### Dipotassium Trioxooxalatomolybdenum (VI) Hydrate

Mentzen et al. (26) reported the singly photochromism of the solid dipotassium trioxooxalatomolybdenum (VI) hydrate. Short periods of irradiation (4 min with UV light) produced a colored species. When heated at 353°K in the dark and in an oxygen atmosphere, the colored species returned to the original color. At longer periods of irradiation, the compound decomposed; however, the evolution of CO<sub>2</sub> showed the resulting photoproduct was not photochromic. The irradiated sample gave an electron spin resonance signal corresponding to molybdenum(V) formation. Other complexes in which Na<sup>+</sup> and NH<sub>4</sub><sup>+</sup> replace the K<sup>+</sup> ions and those containing two or three hydrates were not photochromic.

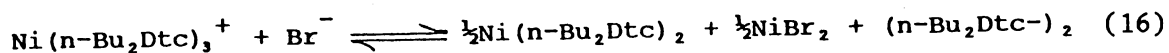
## Ni(IV) Dithiocarbamates

Fackler et al. (27) studied the structure and photoreduction of tris(N,N-di-n-butylthiocarbamato)nickel(IV) bromide. This nickel(IV) complex, shown below, is photochromic in polar organic solvents such as acetone, cyclohexanol, and nitrobenzene, but it is not photochromic in chloroform. It changes from red-brown to pale yellow when irradiated with a projection flood lamp.



Tris(N,N-di-n-butylthiocarbamato)nickel(IV) bromide

A proposed reaction for this thermal bleaching is given by Equation 16. That mechanism is based partly on the fact that the conductivity of the solution drops upon bleaching.



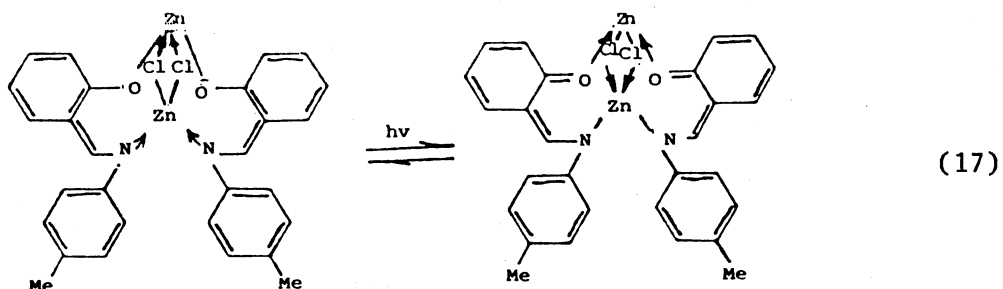
Schwendiman (28) used NMR detection to study the photochromism of the same compound and of the dibenzyl substituted complex. The latter is more soluble and has a slower return reaction which is second order in the total concentration of the Ni(II) species.

In 1979 Eckstein et al. (29) made an ESR investigation of the reversible photoredox reactions of Ni(IV) dithiocarbamates. The substituted complexes included the butyl, benzyl, and cyclohexyl groups, and the anions associated with those complexes were  $\text{ClO}_4^-$  and  $\text{PF}_6^-$ . They reported the second order rate coefficient for  $\text{Ni}(\text{n-Bu}_2\text{Dtc})_3\text{Br}$  is  $5.4 \text{ L mol}^{-1} \text{ sec}^{-1}$ .

## Isomerization

### Zinc Salicylidene-p-Toluidinate

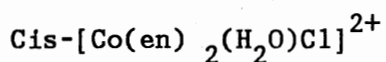
The chelates of beryllium, cadmium, mercury, and zinc with salicylalaniline have been reported (30-32). Only the photochromism of the zinc complex in frozen solutions such as isopentane, isopentene and isopropanol, benzene, and alcoholic solutions was observed. They noted that this photochromic property is observed in ethanol when temperatures are above 175°K. The authors suggested that a valence tautomerism is the mechanism for photochromism and proposed the mechanism given in Equation 17.



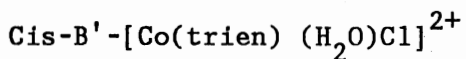
### $K_3[Cr(C_2O_4)_3]$

In 1962 Spee and Adamson (33) followed the decrease in optical activity of  $K_3[Cr(C_2O_4)_3]$  and claimed that photoracemization was the only photochemical reaction. Also they noted that a thermal process produces a racemic mixture. They proposed a mechanism that involves an intramolecular oxalate-oxalate displacement via the hydration of the monodentate intermediate. In 1968 when it was disclosed that irradiating the racemic solution with circularly polarized light increases the optical activity, they said that the reaction is

photochromic (17). But adherence to Adamson's definition does not allow for an intermediate step which this has. Hence this reaction is not photochromic.



In 1974 Adamson and Sheridan (34) reported their findings from the photolysis of  $\text{cis-}[\text{Co}(\text{en})_2(\text{H}_2\text{O})\text{Cl}]^{2+}$ , and in a later publication (6), said it was photochromic. But few observations were reported that to show that the system is photochromic. For example, when the compound was solublized in 0.2 N HCl at 25°C, the equilibrium ratio of the cis- and trans-forms was 73 to 27. A 10 to 90 ratio in a photolyzed solution relaxed to the equilibrium ratio. The authors, however, mentioned that longer irradiations eventually led to further special changes, which were not described. The critical question is, does irradiation of the same solutions the second time give the color changes again? This compound is not photochromic by interpretation of the published results.

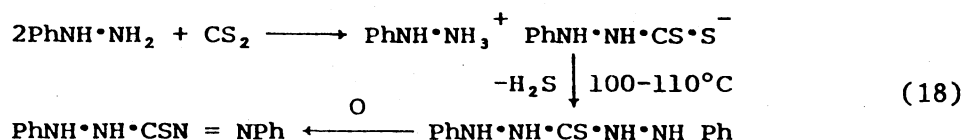


In 1974 Adamson (35) reported that  $\text{cis-B}'\text{-}[\text{Co}(\text{trien})(\text{H}_2\text{O})\text{Cl}]^{2+}$  is photochromic. After irradiation of this form to about 85-90 percent conversion to the trans-form, it returns spectrally on standing in the dark (at 25°C) to the cis-form. Since the thermal equilibrium mixture is essentially 100 percent cis-form, then this describes a photochromic reaction.

## Metal Dithizonates

### Dithizone the Ligand

Dithizone is a bidentate ligand that was first synthesized by Emil Fischer (36) in 1878. He heated carbon disulfide and phenylhydrazine in an organic solvent and then oxidized the products with oxygen in dilute alkali. The following equation gives the reaction.

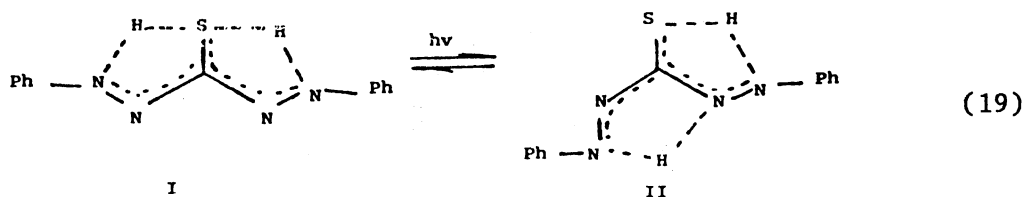


Although its common name is dithizone, other names for it are phenylazothionoformic phenylhydrazide, formazyl mercaptan, and diphenylthiocarbazone. Hellmuth Fischer (37) in 1929 reported that 20 metals react with dithizone to form complexes. The compilations by Iwantscheff (38) and Irving (39, 40) show considerable information has been published about its uses. Dithizone has a chemical formula  $\text{C}_{13}\text{H}_{12}\text{N}_4\text{S}$ , a molecular weight of 256.32, and it forms a violet-black crystalline powder which is insoluble in water at low pH. It is soluble in organic solvents. Its UV-VIS spectrum shows two strong absorption bands near 490 and 605 nm.

Because of the two absorption bands, it was assumed that two tautomers, known as the thione and thiol forms, coexist in solution. More important are the facts that S-methyl derivatives of dithizone and triphenylformazan are photochromic, which is attributed to a trans-cis isomerization (40, 41). Because Meriwether (42, 43) proposed the same mechanism for the metal dithizonates and because the ligand dithizone is

photochromic, it follows that trans-cis isomerization gives the two isomers that eluded previous researchers (42, 44, 45).

Because of the following three facts, Goodwin and Mottola (45) proposed Equation 19 to describe the photochromism of dithizone. Harding (46) reported that the solid reagent had the resonance form like Structure I, Coleman (44) reported that a solution of dithizone in the excited state has Structure II, and Coleman reported that a trans-cis mechanism exists which gives a 5-membered ring compound like the one in the metal dithizonate.



Because the idea of the thiol-thione forms is not universally accepted, the isomers that result from photochromism give an alternative idea (39).

Dithizone contains two active hydrogen atoms, each of which is replaceable by an equivalent of metal. When one hydrogen of the dithizone is replaced, a primary dithizonate is formed. When both are replaced, a secondary dithizonate is formed. Only the primary dithizonates are photochromic (16).

#### Photochromic Dithizonates

The first reference about the photochromic property of a dithizonate is Wichmann's (47) comment in 1940 about W. O. Winkler's recommendations for the determination of mercury using dithizone.



Wichmann wrote, "He (Winkler) indicates that he has at least temporarily abandoned the idea of determining mercury by photometric methods because of the unexplained fluctuations in the reading when the mercury solutions are exposed to the intense light within the photometer." In two succeeding articles Winkler (48, 49) wrote, "It has been observed that the mercury dithizone solution does not come to equilibrium in the photometer immediately, and in most cases the reading will be observed to rise." In the second one he wrote, "...under the influence of a strong light...a rise in the photometric reading...occurred when a filter centered at 610 millimicrons (No. 61) was used, but with a No. 49 filter, there appeared to be a drop in the reading."

Of the 27 metals known to react with dithizone (16), only 16 dithizonate complexes involving 12 metals are photochromic. Table 2 chronologizes these complexes and their references. Webb et al. (50) and Meriwether et al. (42) reported the two mixed ligand complexes; Coleman et al. (51) and Hutton and Irving (52) reported the organo-mercury (II) dithizonates; and Geosling et al. (53) reported one dithizonate. When Ganko et al. (54) used an argon laser to record holograms on solid solutions of Indium (III) dithizonate in polystyrene, they observed that the recorded data had a lifetime of 10 seconds. This demonstrated that indium dithizonate is photochromic.

TABLE 2  
PHOTOCHROMIC METAL DITHIZONATES

Compound	Date	Discoverer	Reference
Hg(HDz) <sub>2</sub>	1940	Winkler	49
HgClHDz	1950	Webb et al.	50
Pd(HDz) <sub>2</sub>	1965	Meriwether et al.	42
Pt(HDz) <sub>2</sub>	1965	Meriwether et al.	42
AgHDz·H <sub>2</sub> O	1965	Meriwether et al.	42
Zn(HDz) <sub>2</sub>	1965	Meriwether et al.	42
Cd(HDz) <sub>2</sub>	1965	Meriwether et al.	42
Pb(HDz) <sub>2</sub>	1965	Meriwether et al.	42
Bi(HDz) <sub>3</sub>	1965	Meriwether et al.	42
Bi(HDz) <sub>2</sub> Cl	1965	Meriwether et al.	42
Ni(HDz) <sub>2</sub>	1965	Meriwether et al.	42
TlHDz	1965	Meriwether et al.	42
CH <sub>3</sub> HgHDz	1966	Coleman et al.	51
In(HDz) <sub>3</sub>	1974	Ganko et al.	54
Cu(HDz) <sub>2</sub>	1978	Geosling et al.	53
PhHgHDz	1979	Hutton and Irving	52

#### Spectral and Chemical Properties

Meriwether et al. (42, 43) reported all the photochromic dithizonates in the ground state have one strong absorption band in the 450-500 nm region, and the absorption maxima for these excited species fall in the 570-620 nm region. As a consequence, the color change usually observed is from orange or red to blue or violet and is independent of the complexed metal. Platinum and palladium dithizonates are exceptions with two absorption bands in the visible region and have color changes of green to yellow. Molar absorptivities for the bands in

the visible region have values near  $10^6$  (M cm)<sup>-1</sup>.

The excitation wavelength region for all the dithizonates is visible light above 450 nm. Varma and Mottola (55) reported a wavelength maximum at 520 nm for silver (I) and mercury (II) dithizonate. While only palladium dithizonate is excited above 640 nm, palladium, silver, mercury, and bismuth dithizonates are excited in the 300-360 nm region. Long periods of irradiation in the 300-320 nm region causes decomposition of the complexes (42).

The chelated metal has little effect on the color of the activated form but has a marked influence on the rate of return to the ground state (42). The half-lives range from about 30 seconds for mercury dithizonate at 25°C to less than 1 second for the cadmium and lead dithizonates at -80°C. The photochromic property, as measured by the return rate in solution, is sensitive to the polarity of the solvent and the presence of acids and bases. The strongest photochromic effects are observed in dry, nonpolar solvents, such as benzene, toluene, chloroform, and carbon tetrachloride. Hydroxylic solvents and organic acids and bases have an accelerating effect on the return of the excited form.

In 1975 Schwendiman (28) found that Hg(II), Pd(II), Bi(III), Ag(II), Ni(II), Tl(II), Zn(II), and Cd(II) dithizonates are not amenable to NMR studies. The reasons given were the majority of the metal complexes are insufficiently soluble, high purity of the complexes is hard to obtain, and the concentration of the excited form is too small to be measured by NMR. Because irradiating light can excite only the molecules on the surface of solid dithizonates, solid NMR can not be used to follow the photochromism.

## Mercury (II) Dithizonate

The photochromism of mercury (II) dithizonate has received the most attention because its slower rate of return is easily followed. While Table 3 is a compilation of values for various physical properties from the work of Schwendiman (28), Meriwether (43), Geosling (53), and Goodwin and Mottola (45), Tables 4 and 5 give additional data for the return rate coefficients. It is apparent that a discrepancy exists in the data for the return rate coefficient and each investigator wrote about its varied effects. For example, Meriwether et al. said that the rate coefficient increases with total concentration of the complex, it increases with water content of the solvent, and it varies with the concentration of active species formed when the sample has not been irradiated to a photostationary state. Yet, Geosling et al. wrote the return rate coefficient was not dependent on the concentration of the complex and there was no large effect due to water in the solvent. She also wrote the coefficient depended on the cleaning of glassware, is not reproducible from run to run, and is subject to dust and other surface catalysis.

Goodwin and Mottola obtained reproducible data when glassware was soaked in a solution of dithizone for one week and when solutions of the mercury dithizonate stored in amber glass bottles are allowed to stand 4 to 20 hours in the dark. They confirmed Geosling's finding that the concentration of the complex does not affect the return rate coefficient. They also found that the rate coefficient depends on the concentration of excess free ligand in the solution, and in the case of a mixed ligand complex of chloride and dithizone, the coefficient depends on the ligand:metal ratio of the mixed ligand complex (56).

Goodwin and Mottola (45) found that a standing time of 4 to 20 hours levels off the effect that water in the solvent has on the rate coefficient. Photoaquation (6) may participate in the photochromism of mercury (II) dithizonate.

TABLE 3  
PHYSICAL VALUES FOR  $\text{Hg}(\text{HDz})_2$

Property	Value	Reference
Forward Rate ( $\text{sec}^{-1}$ )	$1.84 \times 10^{-1}$	28
	$1.33 \times 10^{-1}$	45
Return Rate ( $\text{sec}^{-1}$ )	$2.7 \times 10^{-3}$	43
	$0.5 \times 10^{-3}$	53
	$2.6 \times 10^{-3}$	45
Molar Absorbitivity ( $\text{M}^{-1}\text{cm}^{-1}$ ) of Ground State at 490 nm	$7.0 \times 10^4$	43
	$6.9 \times 10^4$	53
	$6.9 \times 10^4$	45
Molar Absorbitivity ( $\text{M}^{-1}\text{cm}^{-1}$ ) of Excited State at 605 nm at 490 nm	$3.9 \times 10^4$	43
	$2.7 \times 10^4$	53
	$2.6 \times 10^4$	45
Isobestic Points	540 nm	43
	540 and 400 nm	53
	536 and 397 nm	45

TABLE 4  
 THE RETURN RATE COEFFICIENTS FOR DITHIZONATES  
 REPORTED BY MERIWETHER ET AL.

Complex	Solvent	Temp °C	Rate x 10 <sup>2</sup> sec <sup>-1</sup>
Hg(HDz) <sub>2</sub>	Bz	25	1.94
Hg(HDz) <sub>2</sub>	Bz	25	1.72
Hg(HDz) <sub>2</sub>	Bz	25	4.40
Hg(HDz) <sub>2</sub>	Bz	25	2.07
Hg(HDz) <sub>2</sub>	Bz	22	1.17
Hg(HDz) <sub>2</sub>	Bz	25	2.94
Hg(HDz) <sub>2</sub>	Bz	25	0.27
Hg(HDz) <sub>2</sub>	Bz	25	1.06
Hg(HDz) <sub>2</sub>	Bz	22	0.77
Hg(HDz) <sub>2</sub>	Bz	22	1.24
Hg(HDz) <sub>2</sub>	Bz	25	0.13
Hg(HDz) <sub>2</sub>	Bz	25	0.15
Hg(HDz) <sub>2</sub>	Bz	25	0.67
Hg(DDz) <sub>2</sub>	Bz	22	0.25
Ag(HDz)	THF	11.5	1.08
Ag(HDz)	THF	11.5	6.59
Ag(DDz)	THF	11.5	2.42

Bz is benzene and THF is tetrahydrofuran.

TABLE 5  
THE RETURN RATE COEFFICIENTS FOR DITHIZONATES  
REPORTED BY GEOSLING ET AL.

Complex	Solvent	Temp °C	Rate Coefficient sec <sup>-1</sup>
Hg(HDz) <sub>2</sub>	Bz	24	5.3 x 10 <sup>-4</sup>
Hg(HDz) <sub>2</sub>	Bz	24	4.8 x 10 <sup>-4</sup>
Hg(HDz) <sub>2</sub>	Bz	25	1.07 x 10 <sup>-3</sup>
Hg(HDz) <sub>2</sub>	Bz	25	1.23 x 10 <sup>-3</sup>
Hg(HDz) <sub>2</sub>	Bz	45	1.81 x 10 <sup>-3</sup>
Hg(HDz) <sub>2</sub>	Tol	15	4.1 x 10 <sup>-4</sup>
Hg(HDz) <sub>2</sub>	Tol	15	4.5 x 10 <sup>-4</sup>
Hg(HDz) <sub>2</sub>	Tol	15	5.0 x 10 <sup>-4</sup>
Hg(HDz) <sub>2</sub>	Bz	15	9.5 x 10 <sup>-4</sup>
Hg(HDz) <sub>2</sub>	Bz	24	5.0 x 10 <sup>-4</sup>
Hg(HDz) <sub>2</sub>	EtOH	26	9.1
Ag(HDz)	THF	2-3	3.13 x 10 <sup>-3</sup>
Ag(HDz)	THF	29	0.26
Bi(HDz) <sub>3</sub>	DCM	27.7	2.0
Bi(HDz) <sub>3</sub>	DCM	26	1.9
Pb(HDz) <sub>2</sub>	CHCl <sub>3</sub>	25	6.5
Pb(HDz) <sub>2</sub>	DMC	26	4.6
Tl(HDz)	Bz	25	3.8
Cd(HDz)	THF	28	2.3
Cd(HDz)	Acetone	26	86
Zn(HDz)	THF	26	43
Zn(HDz)	DCM	26	7.3 x 10 <sup>-2</sup>
Cu(HDz) <sub>2</sub>	Acetone	26	7.2

Bz is benzene, Tol is toluene, EtOH is ethanol, THF is tetrahydrofuran, DCM is dichloromethane, and CHCl<sub>3</sub> is chloroform.

## Mechanism of Reaction

Meriwether et al. (42) concluded that the reaction was singly photochromic for two reasons. One was that a single isosbestic point that lies between bands of the normal and active forms shows the absence of reaction intermediates. The second was that no thermochromism is detected.

The fact that changes in the infrared spectrum of  $\text{Bi}(\text{HDz})_3$  under irradiation were found analogous to those observed in  $\text{Hg}(\text{HDz})_2$  was taken to mean that the reaction mechanisms of all the dithizonates are the same. Based on his own infrared spectra and on the X-ray crystallographic study by Harding (46), Meriwether assigned Harding's structure of solid  $\text{Hg}(\text{HDz})_2$  as the ground state form in solution. Because no overall chemical change occurs in the photochromic process and the interconversion involves no long-lived reaction intermediates, Meriwether assumed that the activated form of  $\text{Hg}(\text{HDz})_2$  was either an isomer of the normal form or a product formed by the reversible dissociation of the normal form. The dissociation-recombination route was ruled out because the spectrum of free dithizone had never been observed in solutions of the excited complex.

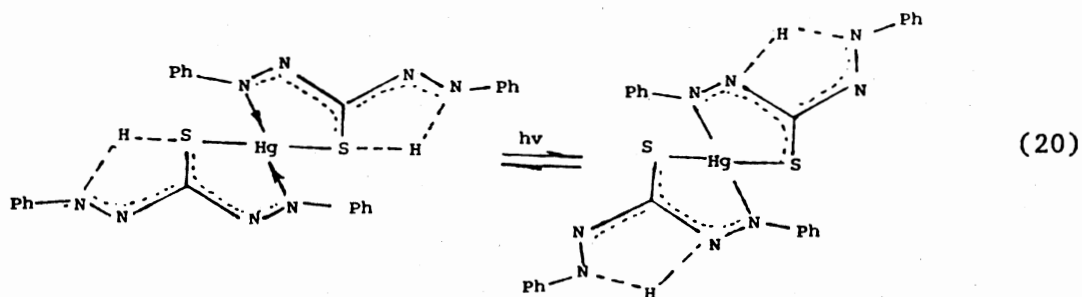
His final assumption was that no direct intramolecular hydrogen transfer from the No. 2 nitrogen atom to No. 4 nitrogen occurs. A water molecule or a second molecule of complex or both must serve as a proton bridge. Meriwether added that the activated complex for this reaction is probably a complex structure consisting of several water and dithizonate molecules bound together by hydrogen bonds. Consequently the photochromic process in metal dithizonates occurs in each ligand independently and is unaffected by the presence of a second or third



dithizone ligand attached to the same central metal atom. He concluded that the mechanism involved a single ligand-metal chelate ring system.

Geosling et al. found configurations of the dithizonates in the excited and ground state are the same for the entire series of dithizonates. She concluded that both ligands isomerize simultaneously. Stereo models of the excited state show that when both ligands isomerize a conjugated bond system that is linked through the mercury atom is formed. Long conjugated systems are known to be blue in color (57).

Considering the above arguments and knowing the ligand is photochromic, Goodwin and Mottola proposed that photochromism of mercury dithizonate involved a trans-cis isomerization of a C--N bond. That photochromic process is given in Equation 20.



The excited state form is a resonance form of the one proposed by Meriwether, and this equation shows that a proton transfer mechanism is not necessary. The mechanisms of reaction for both the dithizone and metal dithizonate involve the same trans-cis isomerization.

#### Substituent Effects on Hg(HDz)<sub>2</sub>

Besides the photochromic dithizonates of Table 2, dithizonates with substituted phenyl rings have been reported. In 1966 Coleman et al.

(51) studied the effect on a number of metal dithizonates by modifying dithizone. Alkyl, fluoroalkyl, alkoxy, and halogen groups that were introduced in the ortho, meta, and para positions of both phenyl rings did not appear to exert a large influence on the forward or return rates of the complexes. Ortho-methoxy groups caused decreases in return rate. The meta substituents have little effect on the wavelength maximum or the molar absorptivities. In the para position, ethyl, chloro, and methoxy groups caused small shifts towards longer wavelengths and small intensity increases. Para fluoro groups had essentially no effect. The largest spectral changes were produced by ortho substituents.

In 1981 Chu et al. (58) investigated the spectral behavior of symmetric and unsymmetric substituted mercury 1,5-diarylthiocarbazonates with trifluoromethyl substitution. They concluded that the large magnitude of the hypsochromic shift produced by the trifluoromethyl substituent is explained by concerted steric and inductive effects, while the smaller bathochromic shift induced by the methoxy substituent is a result of opposing steric and electronic effects. They commented that the proposed photochromic mechanism by Meriwether, which involves a cis-trans isomerization of the azomethine group and a rate determining proton shift, is consistent with their findings.

#### Photochromic Switching

Because Dalberg and Reinganum (59) knew that semiconducting films containing triphenylformazan possess the property of photoconductivity, they showed that  $Zn(HDz)_2$  also contains the same property. They called that property photochromic switching. When the stable, red-colored form is excited to the blue form with an irradiating light, the electric

field present in the surface space charge region ionizes the blue form to a positive charge carrier,  $B^+$ . This  $B^+$  and the photoinjected electron are responsible for the observed photovoltage. This property has utility in photonic switches and erasable optical memories.

### Photochromic Polymers

In 1971 and 1973 Kamogawa (60, 61) reported the results of investigations of three methods of synthesis of photochromic vinyl polymers of the mercury thiocarbazonate series and their properties. He speculated that during the periods of irradiation and relaxation of these polymers, the rates of spectral change were affected by steric conditions, by the chemical structure of the functional groups, and by the comonomer composition.

### Summary

In this chapter photochromism was examined. Its definition was given, as were some of its properties and the different mechanisms that occur in the photochromic processes. Because of interest in photochromic metal-chelates for their potential analytical use, this chapter categorized them by their mechanism. The metal dithizonates were examined because they comprise the largest group of the metal-chelates and have been the most studied photochromic compounds.

## CHAPTER III

### EXPERIMENTAL

#### Equipment

The experimental apparatus used in these studies came from various components. Details are given in Figure 2. Components include an irradiation lamp, 1 (PN 100, 8-V, 50-W, projection lamp, Riluma, Switzerland), with a power supply, 2; an absorptiometric unit consisting of a tungsten lamp, 3 (No. 1439, Chicago Miniature Lamp Works), operated by a regulated power supply, 4 (MP-1026, Pacific Precision Instruments, Concord, CA), a monochromator, 5 (H-10 concave holographic grating, Jobin-Yvon Instrument SA, Inc., Metuchen, NJ), a cell holder, 6, to accommodate a 1-cm glass cell with a battery, 7, to power a magnetic stirring system, 8, and a detector, 9 (HUV-4000B pin photodiode-operational amplifier, EG&G ElectroOptics, Salem, MA), operated by a power supply, 10 (915 Dual Power Supply, Analog Devices, Norwood, MA); a readout unit, 11 (2090A Explorer digital oscilloscope with 94A plug-in and Model D amplifier, Nicolet Instrument Corp., Madison, WI); a signal processor, 12 (Model 7600, Oriel Corp., Stamford, CT); and a controller system consisting of a desktop computer, 13 (9825A, Hewlett-Packard, Palo Alto, CA), with the following Hewlett-Packard peripherals: 9878A I/O expander, 14, 59306A relay actuator, 15, 9885M flexible disk drive, 16, 9871A printer, 17, and 9862A plotter, 17.

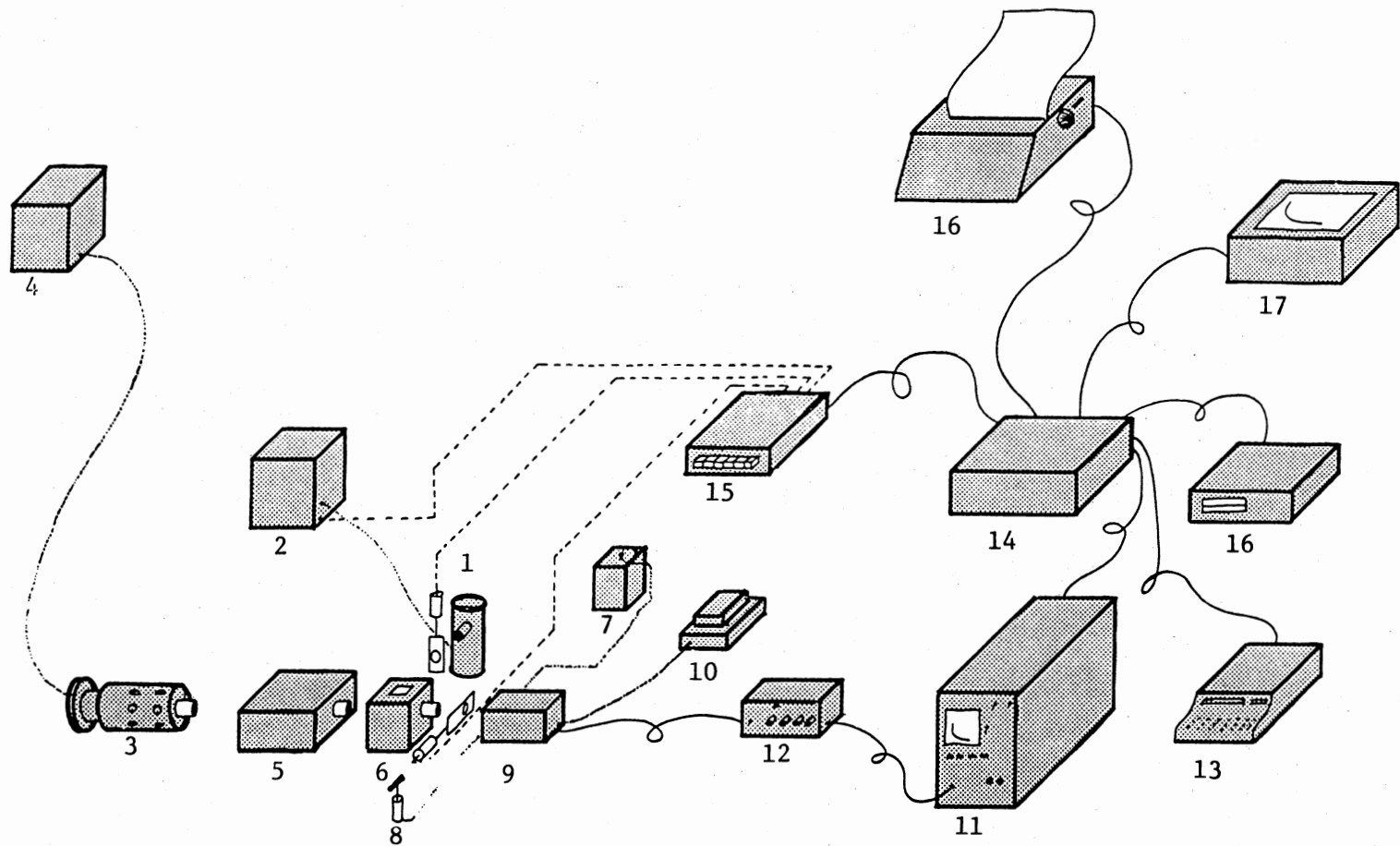


Figure 2. Experimental apparatus used in studies of photochromism.

A constant temperature bath (Lauda/Brinkmann model K2/R Circulator, Brinkmann Instruments Inc., Westbury, NY) circulated water through the water jacket to maintain a constant temperature in the cell holder.

Heat-absorbing glass (6 mm disks, Edmund Scientific Co.) filtered infrared radiation coming from the irradiation lamp. Two shutters that were attached to electrical solenoids controlled the irradiation and protected the detector from the intense light during irradiation.

### Calibrating the Oscilloscope Screen

The readout device for the spectrophotometer was the screen of the digital oscilloscope. The signal from the detector went through the signal processor to the oscilloscope. The signal processor amplified voltages to give full-scale output on the oscilloscope. For example, unless amplified by the signal processor, the detector voltages for the dark current and zero absorbance seldom gave full scale readings on the oscilloscope. Using the signal processor, to set those two output voltages at the beginning of a sample run, made the process of calibrating the instrument quite easy.

That capability of the signal processor had another advantage. It presented an opportunity to expand the absorbance range when monitoring photochromism in samples with high background absorbances. For example, samples with excess ligand often had background absorbances that filled much of the oscilloscope screen. After the screen was calibrated, the signal processor was adjusted such that the background absorbance was at full scale. This expansion of the absorbance scale is called precision photometry; it was implemented into the computer program for collecting data.

## Computer Programs for Data Handling

Two computer programs collected and processed data. The one called FAST4 was a fourth version, and it controlled the experimental spectrophotometer and collected data. It was called "fast" because the program had no reminder statements due to the lack of memory. The program used 31 Kilobytes of the 32K memory available. It was fast at collecting data.

Because of limitations on the size of the computer memory, a second program was written to convert the raw data stored by FAST4 into absorbance values and to print those values on paper. That program was named HRDCP because it made a hardcopy of the data. Listings of the two programs are found in Appendix A.

### Program FAST4

This program assisted the operator in making a sample run. It gave prompts that the operator needed to set up and to initiate a run. Afterwards this program ran the experiment. It irradiated the sample, actuated solenoids, transferred data from the oscilloscope to the computer, and stored data on the floppy disk.

FAST4 contained 108 lines of statements. The first 47 lines were the main program and the remaining were subroutines to the program. The following describes in a general manner the functions of a statement or subroutine in that program.

Lines 1 through 11 created the data and buffer files needed for operation, identified the data file with page and run numbers, and calibrated the instrument. Buffer files received data the computer sent from the oscilloscope. Lines 12 through 26 directed the operator to

place a sample in the spectrophotometer and to input run conditions, such as oscilloscope sweep rate and time for irradiating the sample. Lines 27 through 47 were statements that irradiated the sample and collected the data. These statements also transferred the data from the oscilloscope to the computer memory, helped one to examine and to edit data errors, and then they stored the data on the floppy disk.

The subroutine "CLLCT" in Lines 48 through 53 collected data for a single sweep of the oscilloscope and transferred the data to the computer. "TRNSFR" in Lines 54 through 57 transferred data, and "SUM" in Lines 58 and 59 calculated the average value for the sweep. Average values were calculated for background and zero absorbances and dark currents.

Lines 61 through 70 are the subroutine "SPCTRS." It performed the precision photometry. In addition this subroutine used background information to estimate the oscilloscope sweep rate needed for each sample.

The subroutine "BEEP" alerted the operator with a beep at the end of the waiting period. For example, it gives a beep three seconds before the end of a 60 or 180 irradiations period so the operator did not need a stopwatch. At those times, the operator manually changed sweep rate on the oscilloscope. The switches for various functions of the oscilloscope are not under computer control.

Lines 74 through 89 contain the subroutine "CLEAN." This subroutine allowed the operator to correct an outlier. The subroutine "LINE" allowed the operator to identify and input into the data set those points, such as when irradiation began and ended and what point was the first in the relaxation profile.



The subroutine "WAIT" in Lines 103 through 105 is a timer for a built-in pause. The last subroutine "OPEN" created or opened a new file on a floppy disk and stored the data.

#### Program AMAX-HRDCP

This program converted raw data stored by FAST4 into absorbance units and printed a hardcopy. There were two reasons for the existence of this program. One reason was the computer did not have enough memory for the additional subroutines to operate the instrument. The second was that weekends were set aside for collecting data at the university in Stillwater, Oklahoma, and weekdays were set aside for processing data in Ponca City, Oklahoma.

The computer program consisted of Lines 0 through 34 which specified the data file and the format for printing. Lines 35 through 41 were a subroutine, named "ABSRB1", which printed out all absorbance values in a data file. The printout formatted a table with five columns of data. The subroutine named "ln" calculated the natural logarithm of the absorbance values and printed them out in a second five-column table. Those values were used when processing the data during the weekdays. The subroutine "ABSRB5" in Lines 51 through 58 printed out every fifth absorbance value in a data file. This was an option to the subroutine "ABSRB1". The subroutine "LOGO" in Lines 59 through 77 printed out the heading for the data table. It formatted the information to identify the source of the data, such as run number, irradiation time, background absorbance, and page number in the laboratory notebook.

## Reagents and Solutions

All reagents used were reagent grade. The mercury (II) dithizonate and dithizone came from Eastman Kodak Co., Rochester, NY. The latter was purified as recommended by Irving (39).

## Cleaning of Glassware

All glassware was soaked in 3M hydrochloric acid for approximately one hour, rinsed with distilled water, dried, and filled with a solution of dithizone in benzene. When excess dithizone remained in the glassware after one week, the contents were removed and the glassware was rinsed with solvent, inverted, and air dried. If no excess dithizone remained, then the contents were replaced with a fresh solution of dithizone and conditioning was repeated. After this cleaning procedure, each piece of glassware was marked, used in only one service operation (e.g., a particular pipet was used only to transfer dithizone solutions), and then rinsed with solvent and air dried again.

## Procedures

Solutions involving direct dissolution of mercury dithizonate were allowed to stand 4 to 20 hours in amber glass bottles and in the dark. Afterwards the samples were irradiated and their relaxation to ground state monitored.

Earlier experiments involving mixed solutions of the metal complex with dithizone yielded irreproducible data. The irreproducibility was traced to the variable content of water in the solvent, to the amount of ambient light present during the preparation and transfer of samples, and to the need for a prolonged standing time in the dark. Typically,

4 hours of standing time in the dark was sufficient time to give reproducible results, although standing times of 20 hours were sometimes needed.

Because of these problems, the following procedure was adopted. A series of six samples containing equal concentrations of the dissolved complex and varying concentrations of excess dithizone were prepared in volumetric flasks and transferred to amber glass bottles for storage in the dark. After collecting the data for each sample, the absorbances at 605 nm, for both the background and maximum concentration of the excited species produced, and the observed rate coefficients were examined by plotting. A smooth set of data points indicated stability, and a preponderance of outliers indicated an unstable or contaminated set of samples. These unstable results were discarded.

## CHAPTER IV

### RESULTS AND DISCUSSION

Searching for the variables effecting the photochromism of mercury dithizonate was both satisfying and frustrating. Satisfaction was finding that the equipment worked, that the kinetics of relaxation were first order, and that the excited species was affected by the time of irradiation and the concentration of free ligand. Frustration, however, was finding that data were not reproducible. Absorbance data from consecutive runs of a sample were not identical; there were noticeable changes. The problem seemed to divide itself into two parts. One part was contamination, and the second was the need for a waiting time.

The solution to the problem of contamination was the procedure for cleaning glassware, found in the Experimental Section. That procedure evolved over a period of several weeks. Differences in experimental results, such as absorbances and rate coefficients, depended on the use of new or used amber bottles. When rinsed with solvent, new sample bottles gave better results than used ones. This led to the practice of soaking glassware in a solution of dithizone for one week. It also led to the practice of allocating individual pieces of glassware for one specific service.

With glassware contamination under control, the second problem became more noticeable. It is not yet understood. That is because reproducible results also depended on the amount and type of light where

samples were prepared. For example, when diluting and transferring samples into amber bottles, the amounts of electrical lighting within the room and the ambient light from outside the building caused differences in results. Preparing samples in near total darkness was not a satisfactory solution to that problem. Only when prepared samples were stored in darkness for times ranging from 4 hours to overnight was there help.

In an attempt to monitor this problem with light, two tests were used. Both tests used a series of samples containing increasing amounts of dithizone. The linearity of the plot of background absorbance versus concentration of dithizone became one test for stability. The other test was the smoothness of the plot of the observed rate coefficients versus background absorbance. If either linearity or smoothness were absent, results were disregarded and the waiting time, before collecting another set of data, was extended.

#### Rate Profile Curves

Because the irradiation lamp could overwhelm the detector, absorbance data were not collected during periods of irradiation, only during the relaxation of the excited species. During irradiation, a shutter closed in front of the detector and blocked the light. After irradiation, that shutter opened and a second shutter closed in front of the irradiation lamp to block light coming from the heated filament.

As a consequence, absorbance data, describing a forward rate reaction, came from a series of relaxation experiments. The first absorbance point in a rate profile curve for relaxation became a point in the rate profile curve for the forward reaction. The series of

relaxation curves, from which those first points were taken, differed only in irradiation time.

### The Effect of Dithizone

Whether in excess, in stoichiometric amounts, or in substoichiometric amounts, because dithizone is present, rate profile curves exist. For convenience when studying the changes in curves, the range for the amounts of dithizone is expressed as a ratio of ligand to metal ion. The effects of ligand to metal ion ratio on  $A_{max}$  absorbance and observed rate coefficient are shown in Figures 3 and 4. The  $A_{max}$  absorbance is the difference between background absorbance and the absorbance at the end of irradiation. Those two figures show that the stoichiometric ratio of 2 to 1 produces the maximum absorbance for the excited species and the minimum value for the rate coefficient.

As the amount of excess ligand increases, the maximum absorbances trend to lower values and the observed rate coefficients to higher ones. This suggests the excess ligand absorbs energy during irradiation, and it absorbs energy from the excited species during relaxation. Hence, fewer excited species are produced during irradiation, and they return to the ground state at a higher rate.

As the ratio of ligand to metal falls below two,  $A_{max}$  absorbances trend to lower values, and the observed rate coefficients trend to slightly higher values. This suggests that the ligand absorbs the energy from the light and that the  $A_{max}$  is lower because fewer ligands are present to absorb energy. Because the return rate coefficients are little changed from the one at the stoichiometric ratio suggests no chemical compounds are present to absorb energy from the excited

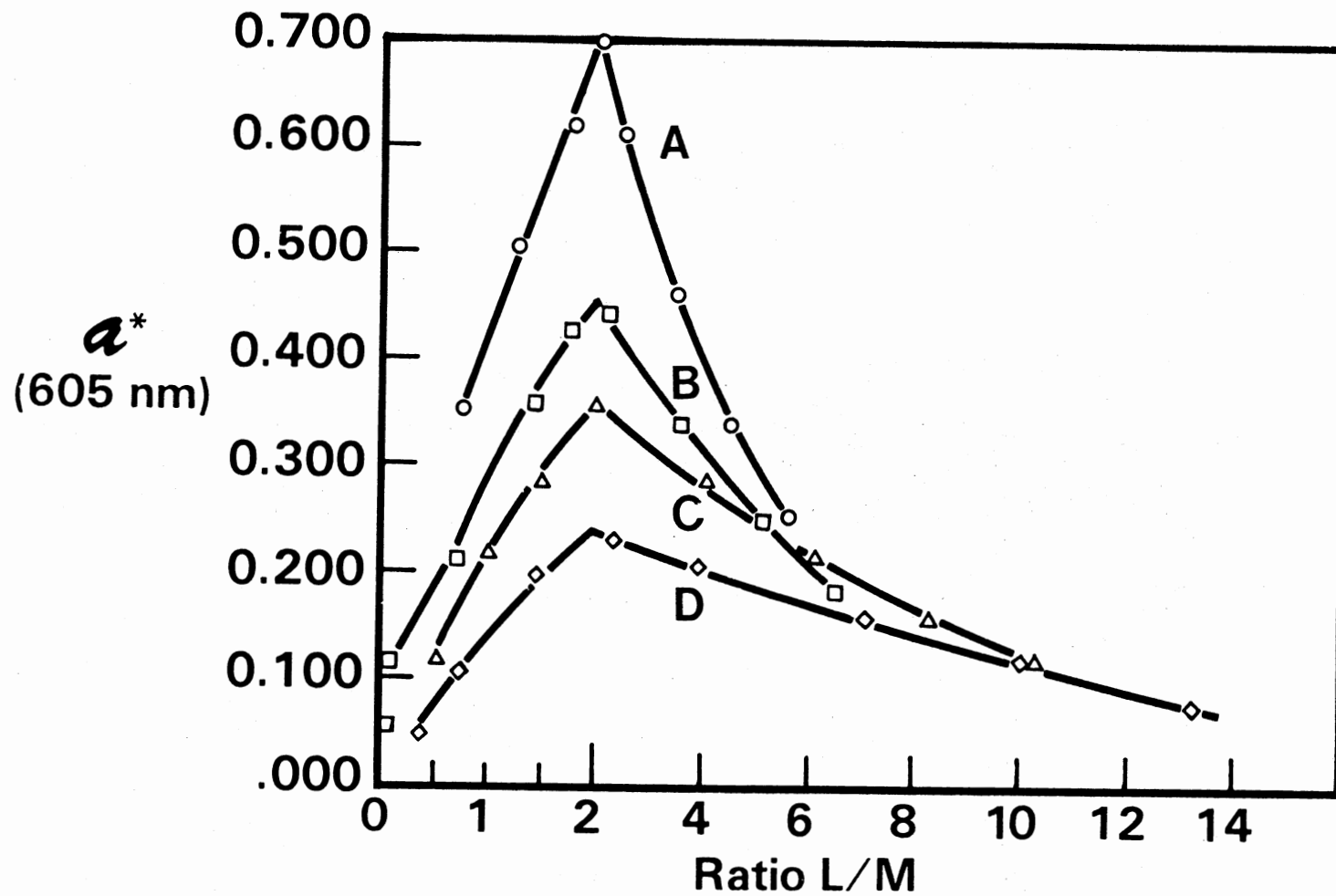


Figure 3. The Excited Species Absorbance as a Function of the Ligand to Metal Ratio

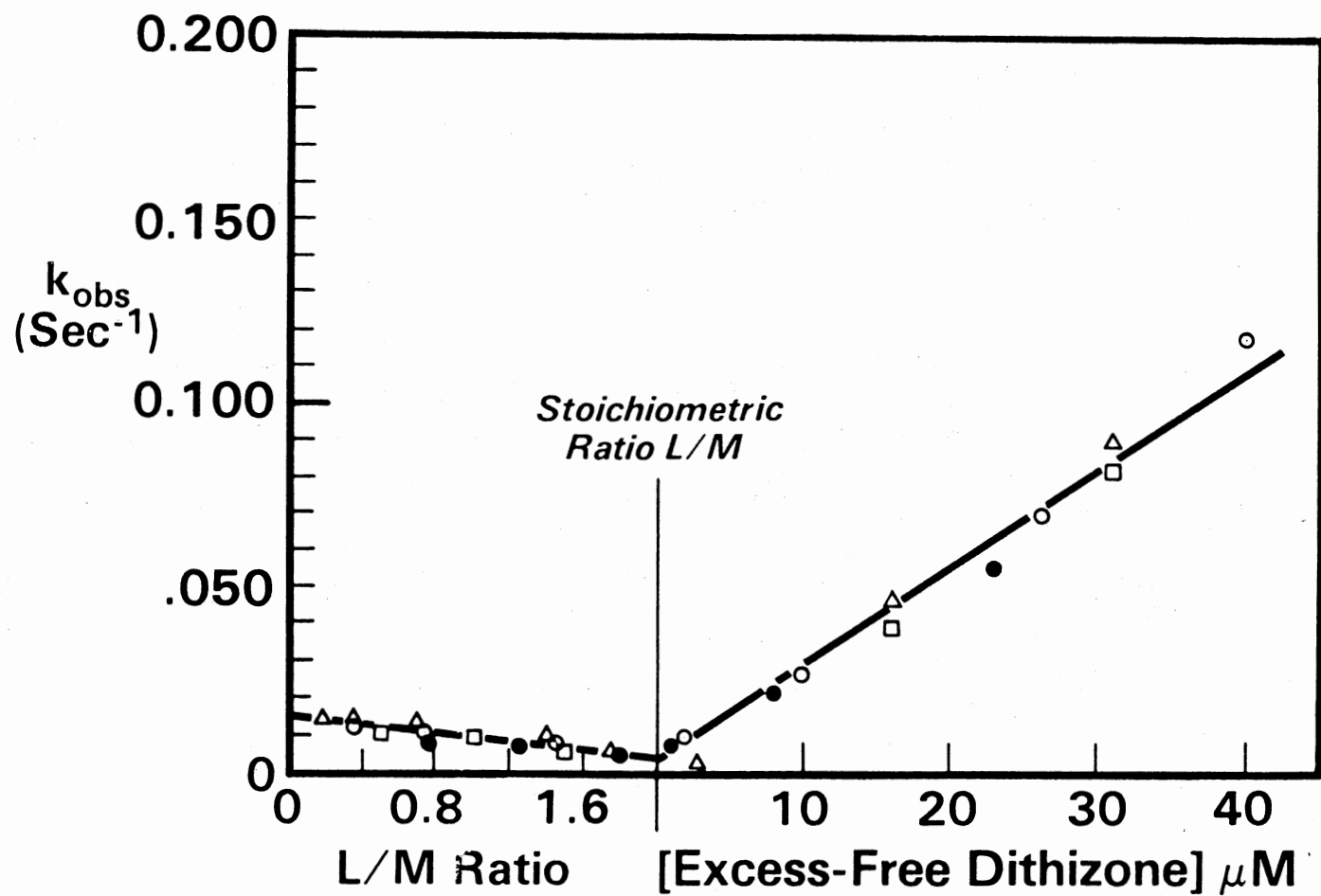


Figure 4. Rate Coefficient as a Function of Dithizone Concentration



species. Hence, the excited species return to ground state like those of mercury (II) dithizonate with the stoichiometric ratio.

#### The Effect of Irradiation Time

When excess ligand was present, the irradiation time effected the rate the excited species returned to the ground. While short irradiation times had no noticeable effect, the longer ones did. For the longer irradiation times, the rates were slow at the beginning of the relaxation process and became faster with time.

The semilogarithmic plots of absorbance versus relaxation time in Figure 5 show those changes. The slopes of those curves are the observed rate coefficients. While the deviations from linearity are more pronounced at the longer periods of irradiation time, a striking feature is the rates became equal as the relaxation progressed.

That fact gave way to speculation about the ligand's role in the relaxation. Speculation was that during irradiation the excess ligand absorbed energy and itself became an excited species. And indeed, dithizone is known to be photochromic. Further speculation was that when in the excited state, the ligand did not help the mercury dithizonate return to its ground state. Only the ground state species of dithizone increased the return rate.

#### Mathematical Model

A mathematical model, accounting for 98.9 percent of the total variation and associating with 302 degrees of freedom, was developed for the photochromism of a mercury dithizonate. That model is:

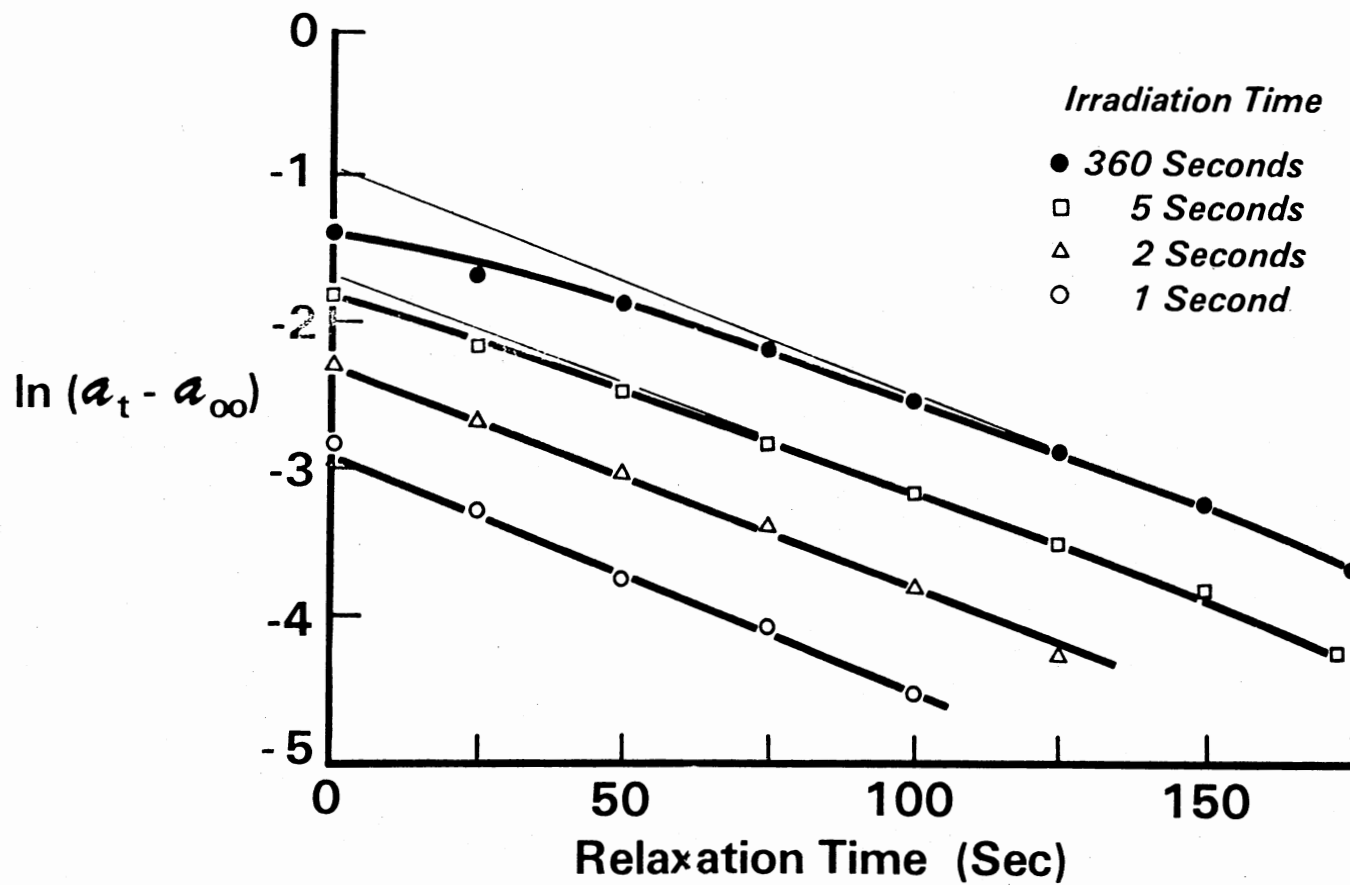


Figure 5. Logarithmic Plot of the Excited Species Absorbance Versus Time

$$A = aC_L + bC_{Hg} * (1 - \exp(-(k_I - k_1 * C_L) * T)) * \exp(-(k_R + k_1 * C_L) * t) \quad (1)$$

where A is absorbance (at 605 nm wavelength), "a" equals 0.9597,  $C_L$  is the concentration of free dithizone, "b" equals 0.0261,  $C_{Hg}$  is the concentration of the mercury dithizonate,  $K_I$  ( $0.1788 \text{ sec}^{-1}$ ) is the forward rate coefficient,  $k_R$  ( $0.0010 \text{ sec}^{-1}$ ) is the return rate coefficient,  $k_1$  ( $0.0904 (C_L * \text{sec})^{-1}$ ) is the rate coefficient for the ligand effect, T is the irradiation time, and t is relaxation time. The concentration unit is micromole.

### Sorting Mathematical Models

Understanding the photochromism of mercury (II) dithizonate came from mathematically modeling the absorbance of the excited species as a function of the complex concentration, the ligand concentration, the irradiation time, and the relaxation time.

Two methods, graphical and numerical, were used to analyze the rate profile curves acquired during relaxation. While the graphical method was initially used, it was abandoned for the latter which used nonlinear regression analysis.

The graphical method was abandoned for two reasons; it was work intense, and it was subject to error. The graphical method typically involved manually plotting on paper the logarithm of absorbance versus time and measuring the slope, the rate coefficient, on the linear plot. Each determination required a separate set of data.

A personal computer, used with the numerical method, offered a distinct advantage: All coefficients in a model were determined simultaneously while using a combined data set consisting of all collected data. This capability permitted the sorting and testing, with

the F-test, of each proposed mathematical model. The acceptance or rejection of each term in the model was based on statistics.

For example, beginning with a simple model such as the following,

$$A = a + bC_{\text{Hg}} \quad (2)$$

where A is absorbance and  $C_{\text{Hg}}$  is the concentration of the mercury dithizonate, one determined the two coefficients, "a" and "b". Adding an exponential function gave the model:

$$A = a + bC_{\text{Hg}} (1 - \exp(-k_I * T)) \quad (3)$$

where  $k_I$  is the rate coefficient for irradiation and T is the time. Using nonlinear regression, one again determined the coefficients.

Since  $k_I$  was preselected at the beginning of the regression analysis, the exponential term introduced only one new variable, T. Because the degrees of freedom in Equation 3 were one less than those in Equation 2, testing the significance of the additional variable was easily performed with the F-test. If the additional variable significantly reduced the total variation of the former model, the variable was kept; if not, the variable was ignored. That approach was used to sort different models in search for the best one.

#### Photochromic Method

An analytical method for the determination of mercury (II) dithizonate in an unknown sample came from the mathematical model.

Knowing the effect of dithizone concentration on absorbance and on the excited species of the dithizonate was the key for developing a simple and practical method. That information allowed one to select boundary conditions for the maximum-allowable dithizone concentration, for the irradiation time, and the relaxation time when taking an absorbance reading.

The maximum-allowable dithizone concentration was arbitrarily selected as that one with a background absorbance equal to 0.500; any concentrations associated with lower backgrounds were acceptable. The practical view was that higher backgrounds would limit or reduce the absorbance range for monitoring the excited species.

The irradiation time, 60 seconds, was a rounded number of the 52 seconds needed to produce 99.9 percent of the total excited-species, when the maximum-allowable dithizone concentration is present. That value of irradiation time simplifies the model by making the exponential term for the forward reaction equal zero.

The relaxation time, zero seconds, was selected as the moment for taking an absorbance reading because zero makes the exponential term for relaxation equal one. This selection of time, as did the 60 seconds for irradiation time in the preceding paragraph, simplifies the model.

When the three limitations are imposed, the mathematical model reduces to the following,

$$A = (a * C_L) + (b * C_{Hg}) \quad (4)$$

where A is the absorbance at 605 nm wavelength determined at the end of irradiation,  $(a * C_L)$  is the background absorbance due to dithizone, and

$(b * C_{Hg})$  is the absorbance due to the excited species.

Rearrangement of this simplified model gives

$$C_{Hg} = (c * A) + (d * C_L) \quad (5)$$

which permits the determination of the concentration of mercury (II) dithizonate in unknown solutions after the coefficients, "c" and "d", are determined from a set of standards. Plotting concentration of dithizonate versus absorbance differences--the difference between total absorbance, A, and background absorbance--gives a calibration curve that can be used in determining the dithizonate.

Twenty data sets were selected from Appendix A to represent standards and unknown samples. The criteria for selecting were the same as those above. A linear regression determined the model's constants, which were used to calculate concentrations of dithizonate.

While Table 6 gives the data used and the concentrations of mercury (II) dithizonate determined, a standard deviation for the twenty samples equaled 0.79. This gave a relative error of 5.3 percent for the determination of mercury (II) dithizonate in that set of samples.

TABLE 6

CONCENTRATIONS OF MERCURY (II) DITHIZONATE: KNOWN  
 CONCENTRATIONS VERSUS THOSE DETERMINED  
 BY PHOTOCHROMIC METHOD

Mercury Dithizonate (Micromoles)	Background (Absorbance)	Measurement (Absorbance)	Calculated Mercury Dithizonate (Micromoles)
20	0.136	0.636	18.3
20	0.136	0.671	19.4
20	0.151	0.729	20.9
20	0.364	0.832	18.9
20	0.253	0.759	19.3
20	0.160	0.733	20.8
20	0.151	0.737	21.1
20	0.132	0.672	19.5
20	0.160	0.733	20.8
20	0.357	0.851	19.7
10	0.074	0.346	10.5
10	0.141	0.382	10.0
10	0.203	0.465	11.1
10	0.185	0.424	10.3
10	0.000	0.257	9.5
10	0.203	0.443	10.4
10	0.202	0.446	10.6
10	0.076	0.308	9.2
10	0.015	0.265	9.4
10	0.133	0.379	10.1

Experimental conditions: Background absorbance < 0.500; Irradiation time, T = 60s; Measurement time, t = 0; Wavelength = 605 nm.

## BIBLIOGRAPHY

1. Marckwald, W., Z. Physik. Chem., 30, 140 (1899).
2. Hirshberg, Y. and Fischer, E., J. Chem. Soc., 629 (1953).
3. Chalkley, L., Jr., Chem. Rev., 6, 217 (1929).
4. Brown, G. H., "Photochromism," in Techniques of Chemistry, Vol. III, G. H. Brown (Ed.), John Wiley and Sons, New York, New York, 1971, Chapter 1.
5. "Photochemistry of Coordination Compounds," V. Balzani and V. Carassiti (Eds.), Academic Press, New York, New York, 1970, 354.
6. "Concepts of Inorganic Photochemistry," A. W. Adamson and P. D. Fleischauer (Eds.), John Wiley and Sons, New York, New York, 1975, 413.
7. Brown, G. H. and Shaw, W. G., Rev. Pure Appl. Chem., 11, 2 (1961).
8. Exelby, R. and Grinter, R., Chem. Rev., 65, 247 (1965).
9. Deb, S. K. and Forrestal, L. J., in Techniques of Chemistry, Vol. III, G. H. Brown (Ed.), John Wiley and Sons, New York, New York, 1971, Chapter 7.
10. Araujo, R. J., in Techniques of Chemistry, Vol. III, G. H. Brown (Ed.), John Wiley and Sons, New York, New York, 1971, Chapter 8.
11. Vernon, L. P. and Ke, B., in Techniques of Chemistry, Vol. III, G. H. Brown (Ed.), John Wiley and Sons, New York, New York, 1971, Chapter 9.
12. Irving, H., Andrew, J. G., Risdon, E. J., J. Chem. Soc., 541 (1947).
13. Bertelson, R. C., in Techniques of Chemistry, Vol. III, G. H. Brown (Ed.), John Wiley and Sons, New York, New York, 1971, Chapter 3.
14. Bertelson, R. C., in Techniques of Chemistry, Vol. III, G. H. Brown (Ed.), John Wiley and Sons, New York, New York, 1971, 974.
15. West, T. S., Chem. and Ind., 1006 (1966).



16. Sandell, E. B. and Onishi, H., "Photometric Determination of Traces of Metals General Aspects," in *Colorimetric Determination of Traces of Metals, Fourth Edition of Part I*, John Wiley and Sons, New York, New York, 1977.
17. Rohly, W. G. and Mertes, K. B., J. Am. Chem. Soc., 102, 7939 (1980).
18. Phillips, J. P., Mueller, A., Przystal, F., J. Am. Chem. Soc., 87, 4020 (1965).
19. Przystal, F., Rudolph, T., Phillips, J. P., Anal. Chim. Acta, 41, 388 (1968).
20. Taylor, L. D., Nicholson, J., Davis, R. B., Tetrahedron Lett., 17, 1585 (1967).
21. Walther D. and Jager, E. G., Z. Chem., 15, 236 (1975).
22. Adamson, A. W., Waltz, W. I., Zinato, E., Watts, D. W., Fleischauer, P. D., Lindholm, R. D., Chem. Rev., 68, 541 (1968).
23. Gafney, H. D. and Adamson, A. W., J. Am. Chem. Soc., 94, 8238 (1972).
24. Bock, C. R., Meyer, T. J., Whitten, D. G., J. Am. Chem. Soc., 96, 4710 (1974).
25. Sima, J., Horvath, E., Gazo, J., Inorg. Chim. Acta, 31, 1460 (1978).
26. Mentzen, B. F. and Sautereau, H., J. Photochem., 15, 169 (1981).
27. Fackler, J. P., Jr., Avdeef, A., Fischer, R. G., Jr., J. Am. Chem. Soc., 95, 774 (1973).
28. Schwendiman, D. P., "Photochromism and Photo-redox Reactions of Metal-Sulfur Chelates," Univ. California, Los Angeles, Calif., 1975, 201 pp. Avail. Xerox Univ. Microfilms, Ann Arbor, Mich., Order No. 76-5129.
29. Eckstein, P., Stach, J., Kirmse, R., Hoyer G., Z. Chem., 18(12), 458 (1978). From Chem. Abstracts, 1979, 90, 112944a.
30. Knyazhanskii, M. I., Gilyanovskii, P. V., Kogan, V. A., Osipov, O. A., Shchipakina, A., Litvinov, V. V., Opt. Spektrosk., 35(6), 1083 (1973). From Chem. Abstracts, 1974, 80, 65213t.
31. Litvinov, V. V., Knyazhanskii, M. I., Osipov, O. A., Kogan, V. A., Rakov, A. S., Gilyanovskii, P. V., Asmaev, O. T., Burlov, A. S., Zh. Prikl. Spektrosk., 20(3), 426 (1974). From Chem. Abstracts, 1974, 81, 56105c.

32. Knyazhanskii, M. I., Gilyanovskii, P. V., Shchipakina, O. A., Osipov, O. A., Litvinov, V. V., Kogan, V. A., Zh. Prikl. Spektrosk., 21(1), 183 (1974). From Chem. Abstracts, 1974, 81, 113067t.
33. Spees, S. T. and Adamson, A. W., Inorg. Chem., 1, 531 (1962).
34. Sheridan, P. S. and Adamson, A. W., J. Am. Chem. Soc., 96, 3032 (1974).
35. Sheridan, P. S. and Adamson, A. W., Inorg. Chem. 13, 2482 (1974).
36. Fischer, E., Liebigs Ann. Chem., 190, 67 (1878).
37. Fischer, H., Zeitschr. fur Angew. Chem., 42, 1025 (1929).
38. Iwantscheff, G., "Das Dithizon und Seine Anwendung in der Mikro-und Spuren-analyse," 2nd (revised) edn., Verlag Chemie, Weinheim, 1972.
39. Irving, H. M. N. H., "Dithizone," The Chemical Society, Analytical Sciences Monographs, Burlington House, London, 1977.
40. Irving, H. M. N. H., "The Analytical Applications of Dithizone," In CRC Crit. Rev. Anal. Chem., 8(4), 321 (1980).
41. Kuhn, R. and Weitz, H. M., Chem. Ber., 86, 1199 (1953).
42. Meriwether, L. S., Breitner, E. C., Sloan, C. L., J. Am. Chem. Soc., 87 4441 (1965).
43. Meriwether, L. S., Breitner, E. C., Colthup, N. B., J. Am. Chem. Soc., 87 4449 (1965).
44. Coleman, R. A., Foster, W. H., Kazan, J. J., Jr., Mason, M., J. Org. Chem., 35, 2039 (1970).
45. Goodwin, A. E. and Mottola, H. A., Anal. Chem., 55, 329 (1983).
46. Hardin, M. M., J. Chem. Soc., 4136 (1958).
47. Wichmann, H. J., J. Assoc. Off. Agri. Chem., XXIII(2), 296 (1940).
48. Winkler, W. O., J. Assoc. Off. Agri. Chem., XXIII(2), 346 (1940).
49. Winkler, W. O., J. Assoc. Off. Agri. Chem., XXIII(2), 310 (1940).
50. Webb, J. L. A., Bhatia, I. S., Corvin, A. H., Sharp, A. G., J. Am. Chem. Soc., 72, 91 (1950).
51. Coleman, R. A., Foster, W. H., Kazaon, J. J., Mason, M., Technical Report 66-9-CM, "Synthesis of Chromotropic Colorants." Contract No. DA19-129-amc-269(N), 1966, United States Army Natick Laboratories, Natick, Massachusetts.

52. Hutton, A. T. and Irving, H. M. N. H., J. Chem. Soc., Chem. Comm., 1113 (1979).
53. Geosling, C., Adamson, A. W., Gutierrez, A. R., Iorg. Chim. Acta, 29, 279 (1978).
54. Ganko, T., Sadlej, N., Smolinska, B. J., Appl. Opt., 13(12), 2770 (1974).
55. Varma, S. R. and Mottola, H. A., Anal. Chim. Acta, 181, 245 (1986).
56. Goodwin, A. E. and Mottola, H. A., unpublished work.
57. Brocklehurst, P. and Burawoy, A., Tetrahedron, 10, 118 (1960).
58. Chu, N. Y. C., Goldstein, S. A., Keehn, P. M., Can. J. Chem., 59, 679 (1981).
59. Dahlberg, S. C. and Reinganum, C. B., J. Chem. Phy., 76(11), 5515 (1982).
60. Kamogawa, H., J. Poly. Sci., 9, 335 (1971).
61. Kamogawa, H. and Watanabe, H., J. Poly. Sci., 11, 1645 (1973).
62. Mueller, J., Leach J. T., Phillips, J. P., Talanta, 10, 1087 (1963).
63. Faller, J. W. and Phillips, J. P., Talanta, 11, 641 (1964).
64. Faller, J. W., Mueller, A., Phillips, J. P., J. Org. Chem., 29, 3450 (1964).

**APPENDIX A**

**COMPUTER PROGRAM FAST4**

```

0: dsp "FAST4--20 Feb 82"
1: dim B[1050];dim YS[2064];buf "data",YS,2;dim AS[6];fxd 0
   ;1+B[1046];0+B[1047]
   ;187+B[1036]
4: if flgl3;jmp -1
5: ent "last rn?",B[1050]
6: if flgl3;jmp -1
7: dsp "slvnt +c11, st .001 s/pt & CNTNU";wtc 2,2;stp
8: dsp "set range & CNTNU";4+B[1029];stp
9: wtc 2,3;gsb "CLLCT"
10: D+B[1026];prt "100%L =",B[1026]
11:
12: dsp "smpl+c11 & CNTNU";wtc 2,2;stp
13: enp "time?",T
14: if flgl3;jmp -1
15: 120+W;gsb "WAIT"
16: gsb "SPCTRS"
17: wtc 2,2
18: ent "SWP FCTR",B[1027]
19: if flgl3;jmp -1
20: ent "SWP-T(sec)",B[1028]
21: if flgl3;jmp -1
22: ent "lite sec",B[1035]
23: if flgl3;jmp -1
24: if B[1035]/(B[1027]*B[1028])>300;sfg 2;beep;beep;beep
25: wtc 2,2;wtc 2,3
26:
27: dsp "ready?--CNTNU";stp
   ) B[1027]*B[1028]*100+W;gsb "WAIT"
29: cmd 7,"?U1","A13";wait 100;cmd 7,"?U1","A2";if flg2;gto 32
30: B[1035]+W;gsb "WAIT"
31: gto 33
32: gsb "BEEP"
33: cmd 7,"?U1","B23";wait 50;cmd 7,"?U1","B1";wait 1075.26
34: ent "Run OK? 1/0",N
35: if flgl3;jmp -1
36: if N=0;gto 7
37: gsb "TRNSFR"
38: ent "data OK? 1/0",N
39: if flgl3;jmp -1
40: if N=0;gsb "CLEAN"
41: gsb "LINE"
42: B[1050]+1+B[1050]
43: gsb "OPEN"
44: files *;asgn AS,l;sprt 1,B[*],"end"
45: for I=1 to 4;spc ;next I;gto 7
46:
47:
48: "CLLCT":wtc 2,2;wtc 2,3;3+W;gsb "WAIT"
49: cmd 7,"?U1","B1";wait 100
50: gsb "TRNSFR"
51: gsb "SUM"
52: ret
5
5 ) "TRNSFR":wtc 2,3;wtc 2,0;wait 75;tfr 2,"data",2064;wtc 2,3
55: for I=0 to 1023;itf(YS[2I+1,2I+2])+B[I+1];next I
56: tfr "data",2;wtc 2,3;ret
57:
58: "SUM":0+D;for I=1 to 1024;B[I]+D+D;next I
59: D/1024+D;ret
60:
61: "SPCTRS":cmd 7,"?U1","A1";wait 100;wtc 2,3;wtc 2,2;gsb "CLLCT"
62: D+B[1025];prt "0%L(HV) =",B[1025];wtc 2,3;gsb "CLLCT"
63: D+B[1031];prt "Aoo-L(HV) =",B[1031];fxd 3
64: prt "Aoo =",-log((B[1031]-B[1025])/(B[1026]-B[1025]))
65: .6933/(-log((B[1031]-B[1025])/(B[1026]-B[1025]))) * 30/.914*.0028+.0026)
66: prt "sec/pt =",3.5*H/650
67: prt "sec/pt =",7*H/650;fxd 0
   ) wtc 2,2;dsp "Set Range";stp ;4+B[1030]
   ) 1+B[1049];ret
70:
71: "BEEP":B[1035]-3+W;gsb "WAIT"
72: for I=1 to 3;beep;beep;wait 1075.26;next I;cfg 2;ret

```

```

73:
74: "CLEAN":enp "move pt #",N
75: if flgl3;jmp -1
76: ent "+ pt #",M
77: if flgl3;jmp -1
78: B[M+1]+B[N+1]
79: ent "nxt mv? 1/0",N
80: if flgl3;jmp -1
81: if N=1;gto 74
82: ent "bd slp? 1/0",N
83: if flgl3;jmp -1
84: if N=0;0+B[1041];gto 88
85: ent "slp tp?",N
86: if flgl3;jmp -1
87: N+B[1041]
88: ret
89:
90: "LINE":ent "N-last Aoo-L pt?",N
91: if flgl3;jmp -1
92: 0+D;for I=1 to N+1;B[I]+D+D;next I
93: D/(N+1)+B[1032]
9 ) prt "Aoo-L(LV) =",B[1032]
95: ent "N-last 0%L pt?",M
96: if flgl3;jmp -1
97: 0+D
98: for I=N+2 to M+1;B[I]+D+D;next I
99: D/(M-N)+B[1040]
100: prt "0%L(LV) =",B[1040]
101: N+B[1037];M+B[1038];ret
102:
103: "WAIT":for I=W to 1 by -1;wait 1075.26;dsp I-1;next I
104: dsp "BLAST OFF";ret
105:
106: "OPEN":prt "Nw f-#",B[1050];spc ;spc ;ent "enter file #",AS
107: asgn AS,1,0,H;open AS,33;dsp AS,"was opened";wait 1000
108: prt "data + dsk";ret
*31064

```

APPENDIX B

COMPUTER PROGRAM AMAX-HRDCP

```

1: dsp "AMAX finds Amax & prnts HRDCP. 13 Mar 82"
2: dim B[1050];dim C[5];dim R[6];dim A$[2];files *
3: ent "what file?",A$
4: if flgl3;jmp -1
5: asgn A$,1,0,H
6: sread 1,B[*]
7: gsb "DELTA"
8: 1024-B[1038]+L
9: fmt 1,20x,"pt #",14x,"ABSORBANCE DATA"
10: fmt 2,f24.0,f8.3,f8.3,f8.3,f8.3,f8.3,f8.3
11: fmt 3,20x,"pt #",16x,"-ln(At - Aoo)"
12:
13: gsb "AMAX"
14: dsp "adjust PRINTER & CNTNU";stp
15: wrt 10;wrt 10;gsb "LOGO"
16: gsb "ABSRB5"
17: wrt 10;wrt 10;wrt 10;wrt 10;gsb "ln"
18: gto 2
19:
20:
21: "AMAX":spc ;spc ;spc ;fxd 0;prt "          pg",B[1036]
22: prt "          run#",B[1050]
23: prt "          irr",B[1035]
24: fxd 3;prt "          Aoc",B[1031]
25: fxd 2;prt "          [EFL]",30/.914*B[1031]
26: gsb "Ao"
27: fxd 0;prt "          lo pt",P;prt "          hi pt",Q;fxd 3
28: prt "          Ao",B[1]-B[1031]
29: prt "          Amax",D;spc ;spc ;ret
30:
31:
32: "ln":0+N;1+X;wrt 10.3
33: for I=1 to L by 10
34: -ln(B[I]-B[1031])+C[X];if C[5]<-6;sfg 5
35: if X=5;wrt 10.2,I-41,C[1],C[2],C[3],C[4],C[5];0+X;N+1+N
36: X+1+X;if N=5;wrt 10;0+N
37: if flg5;cfg 5;gto 2
38: next I;ret
39:
40:
41: "ABSRB5":0+N;1+X;wrt 10.1
42: for I=1 to L by 10
43: B[I]+C[X]
44: if X=5;wrt 10.2,I-41,C[1],C[2],C[3],C[4],C[5];0+X;N+1+N
45: X+1+X;if N=5;wrt 10;0+N
46: next I;ret
47:
48:
49: "LOGO":
50: fmt 4,31x,"#pts",4x,"Aoo",2x,"IRR",2x,"sec/pt",2x,"Page #"
51: fmt 8,24x,"Amax",4x,"[Hg(HDz)2]",3x,"[excess L]",3x,"Run #"
52:   {fmt 5,30x,f5.0,2x,f5.3,x,f4.0,3x,f5.3,3x,f5.0
53:   {fmt 9,23x,f5.3,22x,f5.2,3x,f5.0
54: wrt 10.4
55: wrt 10.5,1024-B[1038],B[1031],B[1035],B[1027]*B[1028],B[1036]
56: wrt 10
57: wrt 10.8
58: wrt 10.9,D,30/.914*B[1031],B[1050]
59: wrt 10
60: wrt 10
61: ret
62:
63:
64: "DELTA":B[1038]+2+C+N;0+D
65: if B[1049]=1;gsb "N-100%L"
66: for I=C to 1024;B[I]-B[1025]+T
67:   -log(T/(B[1026]-B[1025]))+B[I+1-C];next I
68: for I=1031 to 1032;-log((B[I]-B[1025))/(B[1026]-B[1025]))+B[I]
69: next I
70:
71:

```



```

72: "N-100%L":
73: (B[1032]-B[1040])*(B[1026]-B[1025])/(B[1031]-B[1025])+B[1040]+B[1026]
74: B[1040]+B[1025];B[1032]+B[1031];ret
75:
76:
77: "Ao":21+M+D;for T=10 to 30 by 10;if T=20;31+M
78: if T=30;41+M
79: for U=M to 121 by 10
80: for I=1 to 6;0+R[I];next I
81: for I=T to U;I*B[1027]*B[1028]+R[1]+R[1]
82: (I*B[1027]*B[1028])^2+R[2]+R[2];ln(abs(B[I]-B[1031]))+R[3]+R[3]
83: I*B[1027]*B[1028]*ln(abs(B[I]-B[1031]))+R[5]+R[5];next I
84: fxd 3;(R[5]-R[1]*R[3]/(U+1-T))/(R[2]-R[1]^2/(U+1-T))+R[6]
85: R[3]/(U+1-T)-R[6]*R[1]/(U+1-T)+B[1045];exp(B[1045])+N
86: if N<D;N+D;T+P;I+Q
87: next U;next T;ret
*26166

```

**APPENDIX C**

**DATA USED FOR MODELING PHOTOCHROMISM**

<u>a</u>	<u>b</u>	<u>c</u>	<u>d</u>	<u>e</u>	<u>f</u>
background	concentration	irradiation	relaxation	absorbance	calculated
dithizone	MERCURY (II)	time	time	(605 nm)	absorbance
(absorbance)	DITHIONATE	(seconds)	(seconds)		
	(micromoles)				
0.135	20	360	0	0.634	0.651
0.135	20	360	25	0.507	0.504
0.135	20	360	50	0.398	0.398
0.135	20	360	75	0.320	0.323
0.135	20	360	100	0.260	0.268
0.135	20	360	125	0.219	0.229
0.135	20	360	150	0.187	0.201
0.135	20	360	175	0.169	0.181
0.135	20	360	200	0.158	0.166
0.135	20	360	225	0.146	0.156
0.135	20	360	250	0.143	0.148
0.132	20	120	0	0.634	0.648
0.132	20	120	25	0.513	0.504
0.132	20	120	50	0.408	0.399
0.132	20	120	75	0.324	0.324
0.132	20	120	100	0.263	0.269
0.132	20	120	125	0.218	0.230
0.132	20	120	150	0.190	0.201
0.132	20	120	175	0.168	0.180
0.132	20	120	200	0.154	0.165
0.132	20	120	225	0.145	0.154
0.132	20	120	250	0.141	0.147
0.136	20	60	0	0.636	0.652
0.136	20	60	25	0.521	0.504
0.136	20	60	50	0.423	0.398
0.136	20	60	75	0.341	0.322
0.136	20	60	100	0.284	0.268
0.136	20	60	125	0.238	0.229
0.136	20	60	150	0.205	0.201
0.136	20	60	175	0.182	0.181
0.136	20	60	200	0.168	0.166
0.136	20	60	225	0.157	0.156
0.136	20	60	250	0.151	0.149
0.129	20	40	0	0.627	0.644
0.129	20	40	25	0.507	0.503
0.129	20	40	50	0.410	0.400
0.129	20	40	75	0.330	0.325
0.129	20	40	100	0.268	0.270
0.129	20	40	125	0.227	0.230
0.129	20	40	150	0.194	0.201
0.129	20	40	175	0.171	0.180
0.129	20	40	200	0.158	0.164
0.129	20	40	225	0.146	0.153
0.129	20	40	250	0.142	0.145
0.133	20	20	0	0.589	0.630
0.133	20	20	25	0.483	0.490
0.133	20	20	50	0.388	0.389

<u>a</u>	<u>b</u>	<u>c</u>	<u>d</u>	<u>e</u>	<u>f</u>
0.133	20	20	75	0.316	0.316
0.133	20	20	100	0.261	0.264
0.133	20	20	125	0.221	0.226
0.133	20	20	150	0.195	0.198
0.133	20	20	175	0.175	0.178
0.133	20	20	200	0.161	0.164
0.133	20	20	225	0.151	0.154
0.133	20	20	250	0.147	0.146
0.135	20	10	0	0.516	0.552
0.135	20	10	25	0.408	0.433
0.135	20	10	50	0.329	0.347
0.135	20	10	75	0.271	0.286
0.135	20	10	100	0.228	0.242
0.135	20	10	125	0.197	0.210
0.135	20	10	150	0.177	0.187
0.135	20	10	175	0.163	0.171
0.135	20	10	200	0.151	0.159
0.135	20	10	225	0.146	0.151
0.135	20	10	250	0.142	0.144
0.133	20	5	0	0.410	0.422
0.133	20	5	25	0.315	0.340
0.133	20	5	50	0.260	0.281
0.133	20	5	75	0.220	0.236
0.133	20	5	100	0.192	0.207
0.133	20	5	125	0.172	0.185
0.133	20	5	150	0.158	0.169
0.133	20	5	175	0.147	0.157
0.133	20	5	200	0.143	0.149
0.133	20	5	225	0.139	0.143
0.133	20	5	250	0.136	0.138
0.134	20	3	0	0.336	0.333
0.134	20	3	25	0.261	0.276
0.134	20	3	50	0.221	0.234
0.134	20	3	75	0.191	0.205
0.134	20	3	100	0.172	0.185
0.134	20	3	125	0.157	0.168
0.134	20	3	150	0.149	0.157
0.134	20	3	175	0.141	0.149
0.134	20	3	200	0.140	0.143
0.134	20	3	225	0.138	0.139
0.134	20	3	250	0.136	0.136
0.115	20	1	0	0.197	0.191
0.115	20	1	25	0.169	0.171
0.115	20	1	50	0.151	0.155
0.115	20	1	75	0.142	0.144
0.115	20	1	100	0.134	0.136
0.115	20	1	125	0.128	0.129
0.115	20	1	150	0.123	0.124
0.115	20	1	175	0.121	0.121
0.115	20	1	200	0.119	0.118
0.115	20	1	225	0.119	0.116
0.115	20	1	250	0.115	0.114
0.125	20	1	0	0.197	0.200
0.134	20	3	0	0.325	0.333

<u>a</u>	<u>b</u>	<u>c</u>	<u>d</u>	<u>e</u>	<u>f</u>
0.133	20	5	0	0.401	0.422
0.135	20	10	0	0.525	0.552
0.133	20	20	0	0.617	0.630
0.129	20	40	0	0.654	0.644
0.136	20	60	0	0.671	0.652
0.132	20	120	0	0.672	0.648
0.136	20	360	0	0.664	0.652
0.158	20	1	0	0.251	0.230
0.158	20	1	0	0.255	0.230
0.161	20	3	0	0.386	0.357
0.160	20	5	0	0.486	0.445
0.161	20	5	0	0.497	0.446
0.157	20	10	0	0.607	0.571
0.151	20	20	0	0.685	0.647
0.151	20	40	0	0.729	0.665
0.151	20	60	0	0.729	0.666
0.160	20	300	0	0.733	0.675
0.372	20	1	0	0.448	0.426
0.372	20	3	0	0.545	0.539
0.37	20	5	0	0.634	0.623
0.366	20	10	0	0.723	0.750
0.367	20	20	0	0.792	0.844
0.372	20	40	0	0.847	0.875
0.364	20	60	0	0.852	0.869
0.375	20	120	0	0.851	0.880
0.369	20	360	0	0.834	0.874
0.26	20	1	0	0.354	0.323
0.257	20	3	0	0.450	0.440
0.267	20	5	0	0.520	0.536
0.255	20	10	0	0.627	0.655
0.255	20	20	0	0.712	0.742
0.255	20	40	0	0.758	0.764
0.253	20	60	0	0.759	0.763
0.263	20	120	0	0.759	0.773
0.252	20	360	0	0.760	0.762
0.074	10	1	0	0.132	0.112
0.074	10	3	0	0.196	0.176
0.074	10	5	0	0.240	0.221
0.074	10	10	0	0.289	0.285
0.076	10	20	0	0.323	0.325
0.072	10	40	0	0.334	0.329
0.074	10	60	0	0.346	0.332
0.075	10	360	0	0.348	0.333
0.139	10	2	0	0.236	0.206
0.136	10	3	0	0.267	0.232
0.137	10	5	0	0.298	0.278
0.138	10	10	0	0.345	0.343
0.135	10	20	0	0.378	0.380
0.143	10	40	0	0.381	0.397
0.138	10	60	0	0.411	0.393
0.141	10	60	0	0.382	0.396
0.138	10	360	0	0.403	0.393
0.140	10	360	0	0.415	0.395
0.211	10	10	0	0.419	0.410

<u>a</u>	<u>b</u>	<u>c</u>	<u>d</u>	<u>e</u>	<u>f</u>
0.206	10	20	0	0.457	0.447
0.206	10	40	0	0.465	0.457
0.203	10	60	0	0.465	0.455
0.202	10	120	0	0.469	0.454
0.205	10	360	0	0.467	0.457
0.177	10	10	0	0.368	0.379
0.187	10	20	0	0.409	0.429
0.177	10	30	0	0.404	0.428
0.181	10	40	0	0.419	0.433
0.182	10	40	0	0.424	0.434
0.185	10	60	0	0.424	0.438
0.185	10	90	0	0.430	0.438
0.004	10	1	0	0.071	0.046
0.000	10	3	0	0.143	0.108
0.004	10	5	0	0.184	0.158
0.000	10	10	0	0.220	0.217
0.000	10	20	0	0.247	0.254
0.001	10	30	0	0.256	0.261
0.000	10	40	0	0.258	0.261
0.000	10	60	0	0.255	0.261
0.000	10	120	0	0.257	0.261
0.158	20	1	0	0.255	0.230
0.158	20	1	0	0.251	0.230
0.161	20	3	0	0.386	0.357
0.161	20	5	0	0.497	0.446
0.160	20	5	0	0.486	0.445
0.157	20	10	0	0.607	0.571
0.151	20	20	0	0.685	0.647
0.151	20	40	0	0.729	0.665
0.151	20	60	0	0.737	0.666
0.160	20	300	0	0.733	0.675
0.001	10	1	0	0.040	0.044
0.002	10	2	0	0.081	0.080
-0.004	10	3	0	0.104	0.105
0.002	10	4	0	0.128	0.135
0.004	10	5	0	0.153	0.158
0.002	10	10	0	0.199	0.219
-0.001	10	15	0	0.218	0.242
0.002	10	20	0	0.234	0.256
-0.001	10	30	0	0.243	0.259
0.001	10	40	0	0.252	0.262
-0.002	10	60	0	0.247	0.259
0.000	10	120	0	0.252	0.261
0.191	10	1	0	0.225	0.221
0.189	10	2	0	0.259	0.253
0.187	10	3	0	0.274	0.279
0.192	10	4	0	0.296	0.307
0.190	10	5	0	0.313	0.326
0.189	10	10	0	0.362	0.390
0.191	10	15	0	0.386	0.420
0.189	10	20	0	0.397	0.431
0.188	10	30	0	0.411	0.438
0.193	10	40	0	0.420	0.445

<u>a</u>	<u>b</u>	<u>c</u>	<u>d</u>	<u>e</u>	<u>f</u>
0.190	10	60	0	0.423	0.442
0.188	10	120	0	0.425	0.440
0.128	10	1	0	0.159	0.162
0.131	10	2	0	0.198	0.199
0.133	10	3	0	0.223	0.250
0.139	10	4	0	0.256	0.259
0.127	10	5	0	0.250	0.269
0.136	10	10	0	0.311	0.341
0.134	10	15	0	0.335	0.367
0.129	10	20	0	0.339	0.375
0.128	10	30	0	0.355	0.381
0.132	10	40	0	0.368	0.387
0.133	10	60	0	0.379	0.398
0.129	10	120	0	0.373	0.384
0.015	10	1	0	0.054	0.057
0.014	10	2	0	0.080	0.091
0.014	10	3	0	0.111	0.121
0.014	10	5	0	0.144	0.167
0.015	10	10	0	0.203	0.231
0.013	10	20	0	0.228	0.266
0.013	10	40	0	0.256	0.273
0.015	10	60	0	0.265	0.275
0.006	10	120	0	0.259	0.267
0.075	10	360	0	0.331	0.333
0.075	10	360	25	0.293	0.286
0.075	10	360	50	0.259	0.248
0.075	10	360	75	0.229	0.217
0.075	10	360	100	0.204	0.191
0.075	10	360	125	0.180	0.170
0.075	10	360	150	0.157	0.153
0.075	10	360	175	0.142	0.138
0.075	10	360	200	0.129	0.127
0.075	10	360	225	0.117	0.117
0.075	10	360	250	0.109	0.109
0.074	10	60	0	0.324	0.332
0.074	10	60	25	0.290	0.286
0.074	10	60	50	0.263	0.248
0.074	10	60	75	0.227	0.217
0.074	10	60	100	0.204	0.191
0.074	10	60	125	0.182	0.170
0.074	10	60	150	0.161	0.153
0.074	10	60	175	0.143	0.138
0.074	10	60	200	0.133	0.127
0.074	10	60	225	0.116	0.117
0.074	10	60	250	0.106	0.109
0.072	10	40	0	0.318	0.329
0.072	10	40	25	0.286	0.285
0.072	10	40	50	0.254	0.248
0.072	10	40	75	0.224	0.217
0.072	10	40	100	0.198	0.192
0.072	10	40	125	0.174	0.171
0.072	10	40	150	0.155	0.153
0.072	10	40	175	0.139	0.139
0.072	10	40	200	0.127	0.127

<u>a</u>	<u>b</u>	<u>c</u>	<u>d</u>	<u>e</u>	<u>f</u>
0.072	10	40	225	0.116	0.117
0.072	10	40	250	0.106	0.109
0.076	10	20	0	0.308	0.325
0.076	10	20	25	0.270	0.280
0.076	10	20	50	0.242	0.243
0.076	10	20	75	0.212	0.212
0.076	10	20	100	0.187	0.187
0.076	10	20	125	0.165	0.167
0.076	10	20	150	0.147	0.150
0.076	10	20	175	0.134	0.136
0.076	10	20	200	0.121	0.125
0.076	10	20	225	0.110	0.115
0.076	10	20	250	0.102	0.108
0.205	10	360	0	0.448	0.457
0.205	10	360	25	0.372	0.356
0.205	10	360	50	0.319	0.294
0.205	10	360	75	0.279	0.256
0.205	10	360	100	0.246	0.233
0.205	10	360	125	0.228	0.218
0.205	10	360	150	0.219	0.210
0.205	10	360	175	0.210	0.204
0.205	10	360	200	0.206	0.201
0.205	10	360	225	0.206	0.199
0.205	10	360	250	0.204	0.198
0.202	10	120	0	0.446	0.454
0.202	10	120	25	0.377	0.354
0.202	10	120	50	0.319	0.292
0.202	10	120	75	0.273	0.254
0.202	10	120	100	0.244	0.231
0.202	10	120	125	0.224	0.216
0.202	10	120	150	0.214	0.207
0.202	10	120	175	0.209	0.202
0.202	10	120	200	0.205	0.198
0.202	10	120	225	0.207	0.196
0.202	10	120	250	0.203	0.195
0.203	10	60	0	0.443	0.455
0.203	10	60	25	0.371	0.355
0.203	10	60	50	0.316	0.293
0.203	10	60	75	0.272	0.255
0.203	10	60	100	0.242	0.231
0.203	10	60	125	0.225	0.217
0.203	10	60	150	0.214	0.208
0.203	10	60	175	0.210	0.203
0.203	10	60	200	0.208	0.199
0.203	10	60	225	0.204	0.197
0.203	10	60	250	0.206	0.196



PART II

THE DETERMINATION OF SURFACE AREAS OF  
CAPILLARY TUBE REACTORS

## CHAPTER I

### INTRODUCTION

In the past, continuous-flow systems have contained enzyme-immobilized reactors with different configurations, such as packed, open tubular (OTR), and single-bead string (SBSR) (1-4). If minimal band broadening were the criteria used for ranking the designs, the best were the SBSR with enzyme immobilized on the walls of the tubing and on the beads.

The materials for the OTR were glass or plastic, and they were often coiled. The glass ones were made of borosilicate glass, and their inside walls were chemically treated to increase surface areas (2-3). A chemical treatment with fluoride ions at an elevated temperature gives a modified surface characterized as whiskers (2-5). The presence of whiskers enhanced the reactor performance because they increased the surface area which resulted in higher local activity of immobilized enzyme. Other OTRs contained control pore glass (CPG) embedded on the inside wall of the plastic tubing. Both Tygon and Teflon plastics were used in their fabrication (4).

An interesting observation is how the configuration of the reactor affects the sensitivity of the enzymatic method. Kojima et al. proposed a model that included design parameters, such as length and inside diameter (6). They used it to enhance the sensitivity of an analytical method. But their model was lacking because it did not consider the

uneven coverage of the immobilized enzyme along the reactor.

To obtain high local activity of immobilized enzyme requires a reactor with a high surface area. Therefore surface area is an important design parameter. This work tells about determining surface areas for various reactors while using a gas adsorption analyzer. It includes the instrument modifications, its run procedure, the design of a gas adsorption cell, and surface area results.

## CHAPTER II

### REACTOR FABRICATION

#### Materials

##### Glass Reactors and Beads

The coiled glass OTRs selected for surface area measurements were good examples of whisker growth inside capillary tubes. The whiskers of the OTRS and the glass beads were produced during treatments with ammonium hydrogen fluoride (2-3, 14).

##### Plastic Tubing Reactors

Both the Teflon and Tygon plastic OTRs were prepared by embedding CPG onto walls (4). When temperatures above 350°C were used with the Teflon, the following procedure was used.

##### Procedure for Embedding Control Pore Glass

CPG was dried in a vacuum oven overnight at 110°C and then packed into the Teflon tubing. The tubing length was 1 to 2 meters, and its inside diameter was 1 millimeter. Handy items used to pack CPG were glass wool, house vacuum, a funnel, and a vibrating tool. A plug of glass wool placed inside the Teflon tube, where the tubing connected with a vacuum line, stopped the flow of CPG beads during the packing process. The vacuum drew or pulled air through the Teflon tube. That

airflow swept the CPG down the funnel stem and into and through the tube to the glass wool plug. A vibrator which was helped by gravity moved and packed the CPG. After the tubing was packed, the house vacuum was disconnected and a second piece of glass wool was inserted into the other end of the tubing. The tubing was returned to the heated vacuum oven and dried.

Because CPG adsorbed moisture during the packing process, a second drying was necessary. If this second drying step was omitted, degassing often proceeded violently when the tubing was returned to the muffled furnace. At temperatures between 350° to 450°C, degassing was violent enough to remove glass plugs and CPG. The reason was pressure built quickly. It ballooned and ruptured the tubing.

Experimentation was necessary to find the furnace temperature where the optimum amount of CPG was embedded. That is because Teflon becomes brittle and decomposes at temperatures above its melting point. Experimentation began at 350°C and increased 25 degrees with each new repeated attempt to embed CPG. Repeating the procedure depended on the condition of the plastic tubing, for example, just how brittle it was. The selection of the final temperature was a judgement call that primarily depended on the brittleness.

## CHAPTER III

### EXPERIMENTAL

#### Equipment

##### Overview

The gas adsorption analyzer used in this work was designed to determine surface areas of powders. Since the manufacturer expected the small samples would be analyzed, he supplied gas adsorption cells with volumes, such as 3.7, 5.6, 9.0, and 16.2 milliliters (mL). When these were used in the determinations, no problems were experienced.

Problems arose, however, whenever a large gas adsorption cell was used. The following sections tell about those problems. Also, those sections explain how modifications to the instrument and to the run procedure solved those problems.

##### Gas Adsorption Analyzer

A nitrogen gas adsorption analyzer (Model Autosorb-6, Quantachrome Corporation, Syosset, NY) was used in this work and is shown in Figure 1. Shields and Lowell described it in their book (7). The analyzer was an automated physical adsorption instrument which provided adsorption and desorption data on as many as six samples simultaneously.

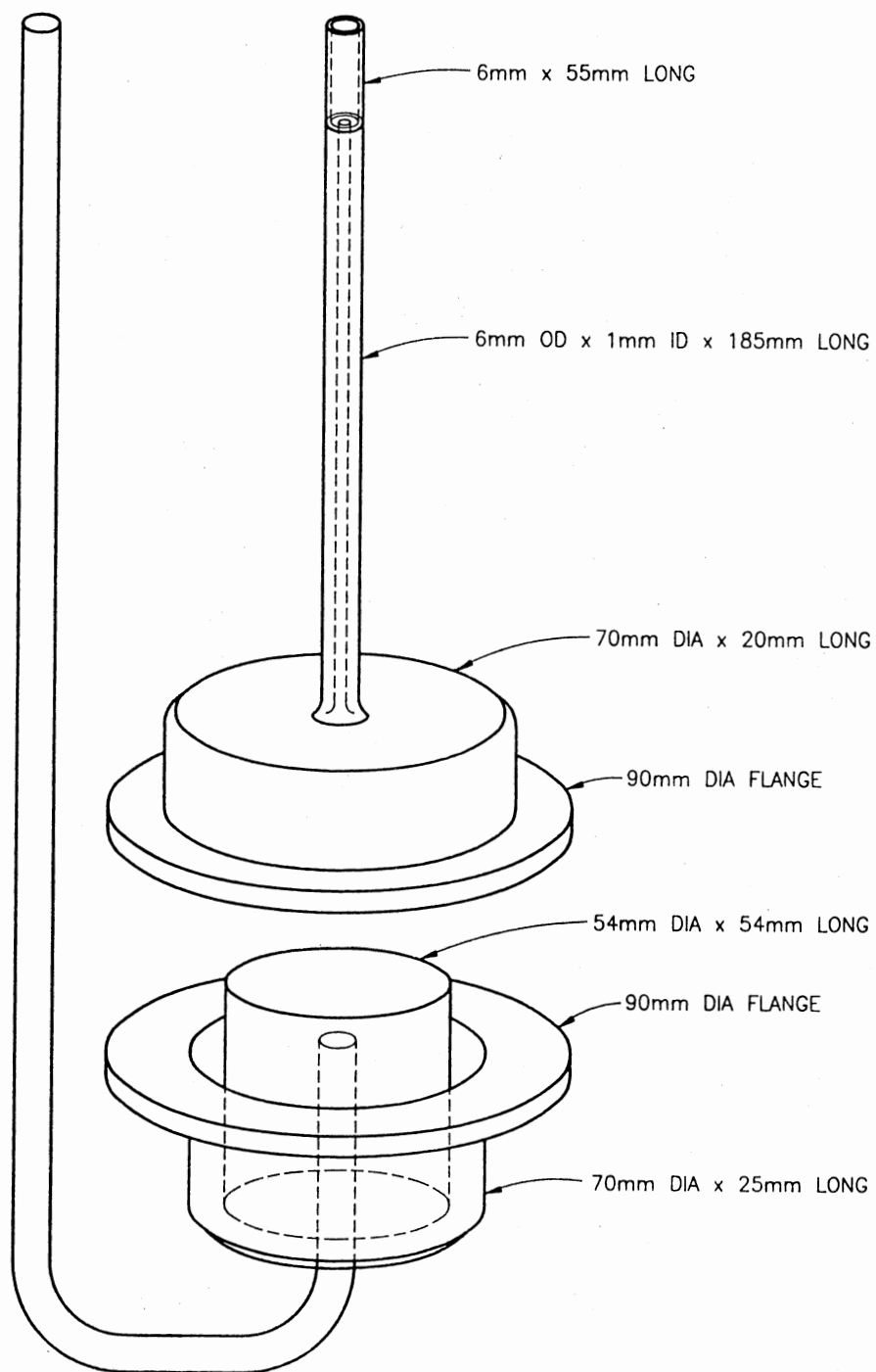


Figure 1. An Automated Gas Adsorption Analyzer for the Determination of Surface Area

It used the static volumetric method in the determinations (8). That method measured quantities of nitrogen gas at various pressures in a fixed volume manifold and added them to the sample cell. These fixed quantities or doses of nitrogen gas are added until a specified equilibrium pressure is reached. Because the sample was held at the temperature of liquid nitrogen, the gaseous nitrogen condensed onto the solid in proportion to the cell pressure. After collecting data at several pressure points, this analyzer processed the data to produce adsorption and desorption isotherms, Langmuir and BET surface areas, pore volume and pore area distributions, and total pore volume (9-13).

#### Gas Adsorption Cell

Because some glass OTRs had coil diameters of 6 centimeters (cm), a large gas adsorption cell was made to hold them. Its volume was 96 mL. Surface areas for a reference material (CPG with a surface area of  $152 \text{ m}^2/\text{g}$ ) differed when determined in cells supplied by the manufacturer from those determined in the large cell.

As an example, when using the manufacturer's cells with the 3.6 mL volumes, typical determinations for surface areas were  $148.0 \pm 1.3 \text{ m}^2/\text{g}$  at the 95 percent confidence interval for four replicates of a reference material. Table 1 gives surface areas for various size samples of CPG that were determined in the large cell. Those results are high, unequal, and exhibited a trend that was inversely proportional to sample size.



TABLE 1  
 SURFACE AREAS FOR VARIOUS WEIGHTS OF CPG  
 IN A LARGE VOLUME (96 mL)  
 GAS ADSORPTION CELL

CPG (g)*	Apparent Surface Area (m <sup>2</sup> /g)
0.0668	1437
0.1000	821
0.1500	505
0.2000	392
0.3500	267
0.3500	266
0.4500	229

\*CPG, mesh size 80/120, surface area 152.7 M<sup>2</sup>/g,  
 ELECTRO-NUCLEONICS, INC., Fairfield, New Jersey.

That trend suggested that the latter values were a function of cell volume. To obtain reproducible results, however, changes in the cell design, modifications to the instrument, and changes in run procedure were made.

Design of Gas Adsorption Cell

Design changes reduced the volume and the mass of the 96 cc cell. These included using a sealed glass jar to reduce the internal volume, replacing the glass stem of the cell with a piece of capillary bore tubing, and cutting down the height of the cell body.

A small sealed glass jar that contained a vacuum was used to reduce the internal volume. In succeeding designs, the jar was molded into the base of the cell, and portions of the bottom surfaces of both the jar and the cell were removed. In the final design of the cell, the interior wall of the jar was exposed to the liquid nitrogen. See

Figure 1 for dimensions of the gas adsorption cell.

Although this design reduced the dead volume of the cell as much as 60 cc, it featured a cavity that held a pocket of gaseous vapor. That pocket of air and nitrogen vapor was a shortcoming. It contributed to variable results.

When the cell was submerged in liquid nitrogen, a pocket of vapor kept the liquid nitrogen away from the inside walls of the jar. Hence the cell and the sample did not reach the temperature of liquid nitrogen (-193°C) before the computer sequenced to the next step in the procedure. In fact, nitrogen continued to boil away for as long as 20 to 30 minutes.

If the manual mode of operation were used, then results became reproducible. When the instrument was in that mode, any cooling time, such as 5 or 30 minutes, could be selected. Surface areas for four replicates of CPG with weights of 0.05 and 0.10 grams in the large cell (36 cc volume) gave  $156 \pm 6.2 \text{ m}^2/\text{g}$  at the 95 percent confidence interval. Those results are acceptable when compared to the values of Table 1.

#### Vapor Vent

A U-shaped tube made from a 40 by 0.7 cm piece of copper tubing was a further improvement. See Figure 2. It vented the vapors trapped in the cavity to the atmosphere of the room. Venting allowed the liquid nitrogen to fill the cavity more quickly, and the cell temperature equilibrated in less than 10 minutes.

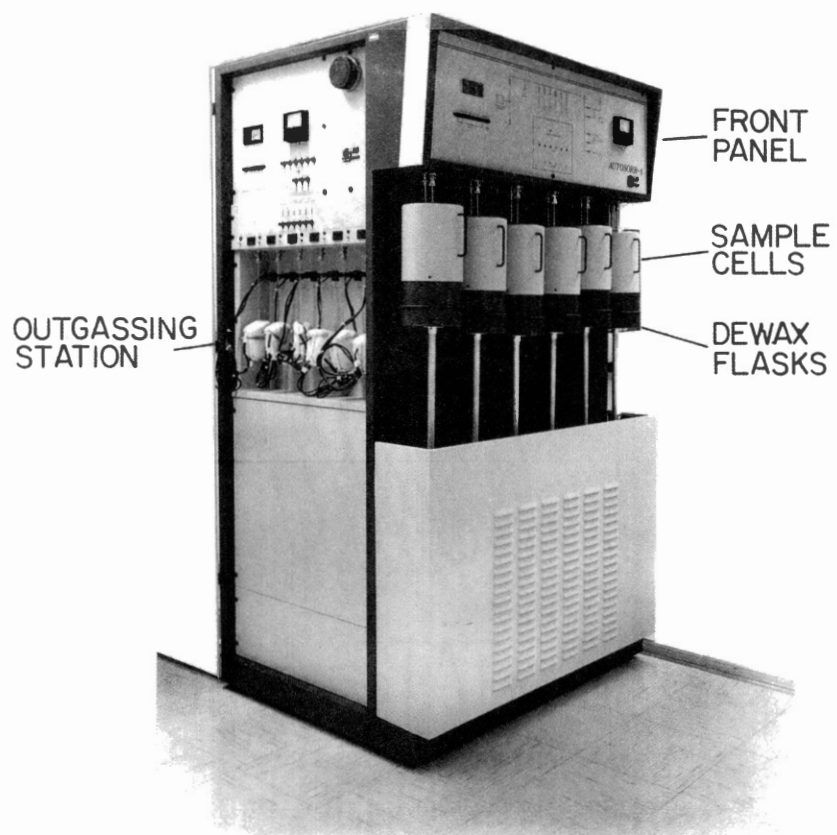


Figure 2. Gas Adsorption Cell for Surface Area Measurements of Capillary Tubes.

## Pressure Surge Filters

The large cell caused an improper calibration of the cell transducer. This problem was traced to the lack of a vacuum in the cell at the beginning of the calibration procedure. At the beginning of each run, the computer calibrates the cell transducer against another transducer in the main manifold. The manufacturer calibrated the main manifold transducer. During the calibration of the cell transducer, outputs of the transducers are compared at several specified pressure points between 0.05 and 1 atmosphere. An improper calibration resulted when the large cell was used.

A vacuum did not exist at the beginning of the calibration procedure. The reason was the instrument could not generate one during a fixed interval of time because of a line filter. The manufacturer had programmed the computer pump-down time for the smaller volume cells. That time was not enough to pump down the large cell.

Line filters are located between the main manifold and each connector port for the six gas adsorption cells. The manufacturer had used filters to reduce pressure surges. A surge occurs when the isolation valve between a sample cell and the main manifold is opened. Frequently the valve is opened when the cell is at atmospheric pressure and the main manifold is under vacuum. On those occasions, surges can carry small particles from the cell into the main manifold. Those particles contaminate the instrument.

To reduce contamination from that source, the manufacturer used line filters with pore diameters of 2 micrometers. With such filters in place, the instrument could not pump a vacuum on a large volume cell during the fixed time interval. The gases diffused too slowly across

the filter for a vacuum to be established in the cell. Because the coiled samples contained no powders, the filter was removed from the line. That corrected the problem.

### Procedure

#### The Blank Correction

The development of the gas adsorption cell revealed variables that effected the cumulative volumes of the isotherm and the run time for analysis. The variables were cooling time, initial temperature of the cell, and two options for instrument settings. The instrument options were EQUILIBRATION TIME with selections that ranged from 1 to 5 and P/Po TOLERANCE with selections that ranged from 0 to 9. The manufacturer suggested settings of 2 and 4 for the two options. A 2<sup>3</sup> factorial-designed experiment determined the level of the effects. See Table 2 for variables and responses levels.

TABLE 2  
VARIABLES AND RESPONSES FOR DETERMINING  
BLANK CELL CORRECTION

Independent Variables	Response Levels	
	+	-
X <sub>1</sub> Initial Cell Temperature (°C)	15	30
X <sub>2</sub> Waiting Time (Minutes)	15	45
X <sub>3</sub> Selected Instrument Setting	(2,4)*	(5,9)

\*(2,4) means the options Equilibration Time = 2 and P/Po Tolerance = 4 were selected. The manufacture suggested these settings.

The results of that experiment indicated the following. A run procedure should use the waiting time of 15 minutes, the lower instrument Options 2 and 4, and the initial cell temperature of 30°C. The reasons for those selections were the 45 minutes waiting time made no difference in results, the instrument options of 5 and 9 unnecessarily extended run time 20 minutes, and the 30°C cell temperature gave better isotherms for the blank run. Those values were better because the cumulative volumes for blanks were constant and near zero. See Tables 3 and 4 for the experimental design and the isotherms. Because the cumulative volumes are not zero implies that a blank correction for each run is necessary.

TABLE 3  
2<sup>3</sup> FACTORIAL DESIGN FOR BLANK CELL

Run No.	Starting Temperature	Waiting Time	Instrument Settings
1	15	15	2,4
2	30	15	2,4
3	15	45	2,4
4	30	45	2,4
5	15	15	5,9
6	30	15	5,9
7	15	45	5,9
8	30	45	5,9

TABLE 4  
 ISOTHERMS FROM THE 2<sup>3</sup> FACTORIAL EXPERIMENT FOR  
 THE BLANK RUNS WITH THE LARGE VOLUME CELL

P/Po	Volume (cc/g)							
	Run 1	Run 2	Run 3	Run 4	Run 5	Run 6	Run 7	Run 8
0.112	-1.04	-1.03	-1.10	-0.86	-1.16	-1.06	-1.00	-0.99
0.165	-1.10	-1.06	-1.13	-0.80	-1.18	-1.12	-1.07	-1.01
0.215	-1.16	-1.06	-1.22	-0.83	-1.22	-1.10	-1.04	-1.05
0.264	-1.19	-1.07	-1.37	-0.81	-1.27	-1.18	-1.10	-1.00
0.314	-1.24	-1.06	-1.36	-0.82	-1.30	-1.27	-1.15	-1.03

The Run Procedure

The following procedure for determining the surface areas evolved out of necessity. The first step was to dry and to degas the reactor overnight in a vacuum oven set at 110°C. Next, the coil was transferred into the gas adsorption cell, and its glass joint was sealed with silicon vacuum grease. The gas adsorption cell was attached to the main manifold, and a vacuum pulled on it while in the manual mode of operation. While the vacuum was being pulled on the cell, a water bath adjusted the cell to the starting temperature of 25°C. That temperature setting was arbitrarily selected in place of the 30°C used in earlier experiments because it was nearer room temperature and because a cell blank correction would be made.

After a period of 5 to 10 minutes, a vacuum was established with less than 5 microns of pressure. The temperature was at equilibrium. At the computer terminal, the operator initiated the run. In the following 10 minutes, the computer calibrated both the pressure

transducer and the cell volume and began raising the bath of liquid nitrogen.

The time required for the bath to rise and to cover the gas adsorption cell with liquid nitrogen was 6 minutes. At the moment the vertical movement of the liquid nitrogen bath stopped and the cell was covered, the operator selected the manual mode of operation for 4 minutes. This gave the delay time needed for the gas adsorption cell and its contents to equilibrate to the temperature of the liquid nitrogen. At the end of this equilibration, the operator returned the instrument to the automatic mode of operation. The computer carries out the remaining steps of the determination. This procedure gave reproducible results.



## CHAPTER IV

### RESULTS AND DISCUSSION

#### Surface Areas

##### Langmuir and BET Methods

Two methods are used for determining surface area, the Langmuir and the BET methods (10, 11). The Langmuir method deals with chemisorption, and the BET method deals with physical adsorption.

The Langmuir method determines the number of molecules that chemically react with a surface. One calculates the surface area by multiplying the number of molecules times the cross-sectional area of the molecule.

BET is an acronym that comes from the first letter of the surnames of Stephen Brunauer, P. H. Emmett and Edward Teller (11). In 1938 they used thermodynamic principles and derived the theory for determining the surface area of a solid. Their theory calculates the number of molecules of a gas that adsorbs onto the surface solid to give a monolayer coverage of a solid. When one knows the cross-sectional area of the molecule and the number of molecules adsorbed, then one can calculate the surface area of the solid.

##### Coiled Glass Reactors

Four coiled glass reactors were selected for BET surface area

determinations. Two coils were equal length pieces that were drawn from the same stock of glass tubing. While Coil 1 was chemically treated to produce whiskers, the blank coil was not. Another coil, designated Coil 2, was selected because it was considered a good example of whisker growth. The last one, Coil 3, was randomly selected from a collection of reactor coils.

Surface area values in Table 5 lie in a narrow range. Three replicate determinations for Coil 1 gave a 95 percent confidence interval of  $0.35 \pm 0.12 \text{ m}^2$ . That statistic is low and indicates nitrogen gas adsorption is not a good method for determining surface areas of these reactors. It cannot determine the irregularity of whisker growth inside a reactor coil.

TABLE 5  
SURFACE AREAS FOR FOUR GLASS COILS

Replicate	Surface Area (sq m)			Blank
	Coil 1	Coil 2	Coil 3	
1	0.50	1.21	0.52	0.27
2	0.41	-	-	-
3	0.22	-	-	-

Significance of the Surface Area Value

To determine how significant the surface area values of the glass coils were, a  $2^3$  factorial design experiment was used. See Table 6 for the treatments and their levels and Table 7 for the experimental design. Two of the three treatments were CPG beads with different weights (0.05 and 0.10 g), which would give surface areas of 7.6 and  $15.2 \text{ m}^2$ ,

respectively. The third treatment consisted of the blank coil and Coil 1.

TABLE 6  
TWO LEVEL FACTORIAL DESIGN FOR 64 mL CELL

Code	Treatment	Treatment Levels	
		-	+
X1	CPG (g)	0.00	0.05
X2	CPG (g)	0.00	0.10
X3	Coil	Blank*	Coil 1

\*Blank is an untreated coil.

TABLE 7  
 $2^3$  FACTORIAL DESIGN FOR DETERMINING  
THE SURFACE AREA OF COIL 1

Trial	Treatment		
	X1	X2	X3
1	0.00	0.00	Blank
2	0.05	0.00	Blank
3	0.00	0.10	Blank
4	0.05	0.10	Blank
5	0.00	0.00	Coil 1
6	0.05	0.00	Coil 1
7	0.00	0.10	Coil 1
8	0.05	0.10	Coil 1

Table 8 gives the five point isotherms that were collected. Their most noticeable features are the negative values for the cumulative volumes of nitrogen adsorbed in Runs 1 and 5. While these isotherms give negative surface areas for the coils, the remaining isotherms give low values for the CPG. But when the data set is analyzed by the Yates

method (15), the surface area results are positive. The Yates method is a mathematical procedure that analyzes data from a factorial-designed experiment. Results for the two treatments of CPG are 155 and 161 m<sup>2</sup>/g, which are near the expected value of 152 m<sup>2</sup>/g. See Table 9 for the worksheet analyzing the isotherms by the Yates method. Because 99.9 percent of the measured effects are attributed to the CPG beads, these results are considered significant. The value for the surface area of Coil 1 (0.27 m<sup>2</sup>/coil) is not significant.

TABLE 8  
ISOTHERMS FOR 2<sup>3</sup> FACTORIAL DESIGN EXPERIMENT  
TO DETERMINE SURFACE AREA OF COIL 1

P/Po	Volume (cc/g)							
	Run 1	Run 2	Run 3	Run 4	Run 5	Run 6	Run 7	Run 8
0.114	-0.58	1.15	3.14	5.14	-0.59	1.15	3.18	5.20
0.165	-0.58	1.30	3.54	5.64	-0.57	1.33	3.51	5.74
0.214	-0.60	1.41	3.84	6.08	-0.60	1.46	3.80	6.17
0.264	-0.62	1.59	4.16	6.49	-0.66	1.59	4.08	6.60
0.314	-0.68	1.70	4.42	6.89	-0.69	1.72	4.31	7.00
CPG (g)		0.0490	0.1001	0.1498		0.0499	0.1000	0.1503

TABLE 9  
CALCULATION OF EFFECTS AND MEAN SQUARES  
FOR COIL 1 BY YATES' METHOD

Run	Surface Area	(1)	(2)	(3)		= Mean square = (3) 2/8 Effect	
---	-1.91	3.25	38.60	78.28	Total		
+-	5.16	35.35	39.68	31.08	4a	120.75	155.40 sq m/g
-+	13.60	3.63	15.22	64.52	4b	520.35	161.30 sq m/g
++	21.75	36.05	15.86	2.16	4ab	0.58	0.54
---	-1.88	7.07	32.1	1.08	4c	0.15	0.27 sq m/coil
+-	5.51	8.15	32.42	0.64	4ac	0.05	0.16
-+	13.79	7.39	1.08	0.32	4bc	0.01	0.08
++	22.26	8.47	1.08	3E-15	4abc	.00	.00
	78.280				TOTAL	641.89	

Surface Areas for CPG Embedded Reactors

To assess the distribution of CPG on the walls of the Teflon tube, surface areas for the whole tube and for a series of segments cut from it were determined. The series came from cutting the tube in half, then selecting one piece and bisecting it, and then selecting one of the resulting segments and bisecting it. This process was repeated for each successive segment until the lengths of the last segments were 1/32 of the original tube length of 2 meters. The surface areas of the whole reactor and of the various segments were made at each step before dividing the next smaller segment. Those data are given in the first part of Table 10. The half of the Teflon reactor that remained as a single piece in the experiment above was segmented, and a series of surface areas similar to the above were made. Those results are given in the second part of Table 10.

TABLE 10

SURFACE AREAS FOR SEGMENTS OF A 2 METER TEFLON  
REACTOR THAT WAS EMBEDDED WITH CPG

	Exper. SA	Embedded Sum of Pieces	With CPG Expect SA	Difference Expected VS Measured	Within 95% CI
1	17.50	17.50	17.537	-0.037	
1	17.80	17.80	17.537	0.263	
1/2	11.60		8.656	2.944	no
1/2	6.42	18.020	8.656	-2.236	no
1/4	4.40		4.215	0.185	yes
3/4	12.90	17.300	13.097	-0.197	yes
1/8	1.13		1.995	-0.865	no
7/8	16.21	17.340	15.317	0.893	no
1/16	0.41		0.885	-0.475	no
15/16	16.20	16.610	16.427	-0.227	yes
1/32	0.07		0.330	-0.260	yes
31/32	18.07	18.140	16.982	1.088	no
1	18.05	18.05	17.537	0.513	
1/2	11.76		8.656	3.104	no
1/2	6.14	17.90	8.656	-2.516	no
1/4	4.86		4.215	0.645	no
3/4	11.71	16.57	13.097	-1.387	no
1/8	2.44		1.995	0.445	no
7/8	14.88	17.32	15.317	-0.437	no
1/16	1.15		0.885	0.265	yes
15/16	15.55	16.70	16.427	-0.877	no
1/32	0.27		0.330	-0.060	yes
31/32	16.21	16.48	16.982	-0.772	no

Average = 17.364

std = 0.607

95% CI = 0.367

The following approach was used to analyze data for the uniformity. The first step was to estimate the 95 percent confidence interval for the error in a surface area measurement. Column 3 of Table 10 gives the surface areas for three replicate determinations of the whole reactor

and for ten combined values. These combined values are the sum of two determinations for the segments. For example, the sum of the surface areas for the 1/4 and 3/4 segments gives a combined value of  $17.3 \text{ m}^2$ . From these 13 values a mean of  $17.36 \text{ m}^2$ , a standard deviation of  $0.607 \text{ m}^2$ , and a 95 percent confidence interval of  $\pm 0.367 \text{ m}^2$  are calculated.

The second step in the assessment was to determine the differences between the expected and experimental surface areas for the segments. While Column 4 of Table 10 gives the expected values for each fractional part, Column 5 gives the differences. The last step in the test was to examine the data in Column 5 to see which data lay within the 95 percent confidence interval. Only 6 out of the 20 segments, or 30 percent, lay in the interval. Because 70 percent of the surface areas were outside the expected limits, that test indicated the distribution of CPG was not uniform.

Another Teflon tube (id 0.7 mm) was embedded with CPG beads for the purpose of increasing its surface area. Through repeated steps of packing, degassing, heating, and unpacking, a final temperature of  $425^\circ\text{C}$  was used for embedding the CPG. Earlier experiments showed that the Teflon tube melted down at  $450^\circ\text{C}$  within 10 minutes. At the final temperature, approximately one-half of the tube became friable and disintegrated with handling. But the remaining piece had a length of 1/2 meter and had a surface area of  $41 \text{ m}^2$ . The results are in Table 11. The same test for the variability in the surface area of the segments indicated that the CPG was evenly distributed in the tube. With a variability of  $2.201 \text{ m}^2$ , only 20 percent of the measurements were outside the test interval,  $\pm 2.038 \text{ m}^2$ .

TABLE 11  
SURFACE AREAS FOR SEGMENTS OF A 1/2 METER TEFLON  
REACTOR THAT WAS EMBEDDED WITH CPG

	Exper. SA	Embedded Sum of Pieces	Expected SA	Difference Expected VS Measured	Within 95% CI
1	41.41	41.41	37.947	3.463	
1	41.36	41.36	37.947	3.413	
1/2	20.24		18.838	1.402	yes
1/2	18.27	38.51	18.838	-0.568	yes
1/2	19.90		18.838	1.062	yes
1/2	16.42	36.32	18.838	-2.418	no
1/4	9.78		9.284	0.496	yes
3/4	28.68	38.46	28.393	0.287	yes
1/8	5.01		4.507	0.503	yes
7/8	31.48	36.49	33.170	-1.690	yes
1/16	1.83		2.119	-0.289	yes
15/16	33.31	35.14	35.558	-2.248	no

Average = 38.241  
std = 2.201  
95% CI = 2.038

Test intervals of  $\pm 0.367 \text{ m}^2$  for the first Teflon reactor and  $\pm 2.04 \text{ m}^2$  for the latter raised concern for the validity of the test. But when one considers the relative errors, 0.035 and 0.058, and the degrees of freedom, 13 versus 7, used to calculate the intervals, then the interpretation of results appears reasonable. While the first reactor lacks a uniform covering of the walls with CPG and the second one has uniformity of covering, this suggests time and temperature are the controlling parameters for optimizing the embedding process. Certainly more CPG per unit length of reactor would allow one to increase the amount of immobilized enzyme. Then one can use shorter length reactors.



## Surface Areas of Glass Beads

A series of glass beads used in fabricating SBSR were selected for surface area measurements. The series of beads were produced by the variety of chemical treatments for increasing surface areas and for preparing the surfaces for the immobilized enzyme. Treatments included using a Soxhlet extractor charged with hydrochloric acid to leach metals from the glass, using saturated solutions or slurries of ammonium bifluoride in methanol to etch the beads that are agitated in a heated sonic bath, and drying the beads in an oven.

All surface areas were less than  $0.1 \text{ m}^2/\text{g}$ , except for those beads that were leached with hydrochloric acid. Their surface areas were approximately  $1 \text{ m}^2/\text{g}$ . Table 12 gives examples of the beads, treatments, and the surface areas determined. As in the case of the coiled glass reactors, one concludes that the gas adsorption analyzer is not a good technique for measuring the surface areas of beads.

## Summary

The gas adsorption analyzer that uses nitrogen gas as adsorbate has limited usefulness when accessing the uniformity of surface areas within capillary tube reactors. Only reactors made by embedding CPG inside a Teflon capillary tube contained sufficient surface areas for measurement. Because segments of these reactors had measurable areas, then their uniformity could be measured. Similar reactors made with Tygon were not measured because the plastisizer covered the CPG during the degassing procedure.

TABLE 12  
CHEMICAL TREATMENTS OF GLASS BEADS

Large Glass Beads and Treatment	Surface Area (sq m/g)	Remarks
Untreated Glass Beads	<0.1	
Untreated Glass Beads	<0.1	
HCl leached	1.0	Soxhlet extraction with conc. HCl to remove metals.
HCl leached	1.2	
HCl leached w/boiling chips	0.6	Used boiling chips in flask.
Etched (4 hrs), leached	<0.1	Slurry of $\text{NH}_4\text{FHF}$ in methanol, then HCl.
Soln etched (8 hrs)	<0.1	Solution of $\text{NH}_4\text{FHF}$ in methanol while heated in sonic bath.
Soln etched (24 hrs)	<0.1	
Etched beads (0.5 MM)	<0.1	Leached with $\text{NH}_4\text{FHF}$ ,
Etched + leached + baked	<0.1	leached with HCl, baked in oven, washed in water.
Etched + leached + baked + wash	<0.1	
Leached + etched + baked	<0.1	Different order for treatments.
$\text{NH}_4\text{FHF}/\text{H}_2\text{O}$ Etched Beads	<0.1	Slurry of $\text{NH}_4\text{FHF}$ in water.

The uniformity of the surface of other reactors, such as OTR and SBSR, that were chemically treated with fluoride ion to produce whisker growth were not measured, because their total surface areas were insignificant when using nitrogen as the adsorbate.

#### Fractal Dimension

The concept of the fractal (noninteger) dimension has recently appeared in the literature (17-19). The fractal dimension measures the irregularity of a surface. Because the surfaces of CPG were not smooth, a question was, Is CPG fractal? The method of Avnir (19) showed that one sample (CPG00075, 200/400 MESH, ELECTRO-NUCLEONICS, INC, Fairfield,

NJ) had a fractal dimension equal to 2.99.

That determination used the following steps. The sample was screened into five fractions. The sieves had the US Sieve designations 170, 200, 230, 270, 325, and M20. See Table 13 for the average particle diameters that come from using that set of sieves. Included in that table are the BET surface areas for each fraction. After constructing a log/log plot of surface area versus diameter of particle, the slope of the line is determined. For that sample, it was near zero. The final step in Avnir's method gave the fractal dimension. It equals 3 plus the slope of the line, i.e.,  $D = 2.99$  for this sample.

TABLE 13  
SIEVE DESIGNATIONS, PARTICLE DIAMETER, AND SURFACE  
AREAS FOR CONTROL PORE GLASS BEADS  
(OSU-CPG00075 200/400 MESH)

Diameter Seive	SA (Micron)	(m <sup>2</sup> /g)	Log(Open)	Log(SA)
170/200	82.0	153.4	1.914	2.186
200/230	68.5	154.9	1.836	2.190
230/270	58.0	153.9	1.763	2.187
270/325	49.0	104.2	1.690	2.010
325/M20	32.5	125.9	1.512	2.100

The fractal dimension of another sample of CPG (OSU-CPG03000 200/400 MESH, ELECTRO-NUCLEONICS, INC, Fairfield, NJ) was measured. It equaled 2.002. Table 14 gives the data that was collected for the sample.

TABLE 14

SIEVE DESIGNATIONS, PARTICLE DIAMETER, AND SURFACE  
AREAS FOR CONTROL PORE GLASS BEADS  
(OSU-CPG03000 200/400 MESH)

Diameter Seive	SA (Micron)	(m <sup>2</sup> /g)	Log(Open)	Log(SA)
170/200	82.0	12.35	1.914	1.092
200/230	68.5	12.28	1.836	1.089
230/270	58.0	24.84	1.763	1.395
270/325	49.0	17.28	1.690	1.238
325/M20	32.5	NA	1.512	NA

While a fractal dimension of 2 indicates a smooth surface, a dimension of 3 indicates an irregular surface. Hence, the surfaces of these samples were different from each other. The surface of the first sample was very irregular, and the surface of the second was smooth.

That finding gave the idea that the fractal dimension could be used to design better chemical reactors. For example, what degree of surface irregularity is best for chemical bonding? Similarly, when the size of a functional group being immobilized changes, does one select a CPG with a different degree of irregularity? Other questions come to mind. For example, does immobilization change the fractal dimension of the CPG? If so, why? Do enzymes and other functional groups have fractal surfaces? Finding answers to these questions will lead to more efficient designs of chemical reactors for flow injection analysis.

## BIBLIOGRAPHY

1. Iob, A., Mottola, H. A., Anal. Chem., 52, 2332 (1980).
2. Iob, A., Mottola, H. A., Clin. Chem., 27, 195 (1981).
3. Gnanasekaran, R., Mottola, H. A., Anal. Chem., 57, 1005 (1983).
4. Gosnell, M. C., Snelling, R. E., Mottola, H. A., Anal. Chem., 58, 1585 (1986); Anal. Chem., 58, 2592 (1986).
5. Onuska, F. I., Comba, M. E., Bistricki, T., and Wilkinson, R. J., J. Chromatogr., 142, 117 (1977).
6. Kojima, T., Hara, Y., Morishita, F., Bunseki Kagaku, 32, E101 (1983).
7. Shields, J. E., Lowell, S., Amer. Lab., 11, 81 (1984).
8. Powder Surface Area and Porosity, S. Lowell and J. E. (Eds.), 2nd Ed., Chapman and Hall, NY, 1984.
9. Langmuir, I., J. Am. Chem. Soc., 38, 2221 (1916).
10. Langmuir, I., J. Am. Chem. Soc., 40, 1361 (1918).
11. Brunauer, S., Emmett, P. H., and Teller E., J. Am. Chem. Soc., 60, 309 (1938).
12. Brunauer, S.; Deming, L. S.; Deming, W. E.; and Teller, E., J. Am. Chem. Soc., 62, 1723 (1940).
13. Barrett, E. P., Joyner, L. G., and Halenda, P. P., J. Am. Chem. Soc., 73, 373 (1951).
14. Gosnell, M. C., Mottola, H. A., Anal. Chem., 58, 631 (1986).
15. Matt Gosnell. Private communication.
16. Design and Analysis of Industrial Experiments, Owen L. Davies (Ed.), 2nd Ed., Hafner Publishing Co., New York, NY, 1967, 264.
17. Avnir, D.; Farin, D. and Pfeifer, P. Nature, 308, 15 Mar 1984, 261-263.

18. Pfeifer, P. and Avnir, D. J. Chem. Phys. 1983, 79(7), 3558-3565.
19. Avnir, D.; Farin, D. and Pfeifer, P. J. Chem Phys., 1983, 79(7), 3566-3571.

VITA

Anton Elbert Goodwin

Candidate for the Degree of

Doctor of Philosophy

Thesis: PART I: THE PHOTOCROMISM OF MERCURY (II) DITHIZONATE AND  
PART II: THE DETERMINATION OF SURFACE AREAS OF CAPILLARY TUBE  
REACTORS

Major Field: Chemistry

Biographical:

Personal Data: Born in Kingfisher, Oklahoma, November 16, 1935,  
the son of Anton Eble and Mary Lucile Goodwin. Married to  
Betty Jean Fackler, December 30, 1964.

Education: Received Bachelor of Arts degree from Phillips  
University in May 1958; received Master of Science degree from  
Oklahoma State University in August 1975; completed  
requirements for the Doctor of Philosophy degree at Oklahoma  
State University in May 1988.

Professional Experience: Member of the American Chemical Society;  
analytical chemist, Doughnut Corporation of America,  
Hillsdale, Michigan, January 1960 to February 1963; analytical  
chemist, Refining Department, Conoco Inc., Ponca City,  
Oklahoma, and Westlake, Louisiana, February 1963 to November  
1968; analytical chemist, Analytical Section, Research  
Services Division, Research and Development Department,  
Conoco Inc., Ponca City, Oklahoma, November 1968 to present.